SHORT-CONTEXT DOMINANCE: HOW MUCH LOCAL CONTEXT NATURAL LANGUAGE ACTUALLY NEEDS?

Anonymous authors

000

001

002

004

006

008 009

010 011

012

013

014

015

016

017

018

019

021

023

025

027 028 029

031

033

034

037

040

041

042

043

044

046

047

048

051

052

Paper under double-blind review

ABSTRACT

We investigate the short-context dominance hypothesis: that for most sequences, a small local prefix suffices to predict their next tokens. Using large language models as statistical oracles, we measure the minimum context length (MCL) needed to reproduce accurate full-context predictions across datasets with sequences of varying lengths. For sequences with 1–7k tokens from long-context documents, we consistently find that 75–80% require only the last 96 tokens at most. Given the dominance of short-context tokens, we then ask whether it is possible to detect challenging long-context sequences for which a short local prefix does not suffice for prediction. We introduce a practical proxy to MCL, called Distributionally Aware MCL (DaMCL), that does not require knowledge of the actual next-token and is compatible with sampling strategies beyond greedy decoding. Our experiments validate that simple thresholding of the metric defining DaMCL achieves high performance in detecting long vs. short context sequences. Finally, to counter the bias that short-context dominance induces in LLM output distributions, we develop an intuitive decoding algorithm that leverages our detector to identify and boost tokens that are long-range-relevant. Across Q&A tasks and model architectures, we confirm that mitigating the bias improves performance.

1 Introduction

When prompted to continue a piece of text, how much preceding context do humans rely on? Do they focus on recent words and local coherence, or plan with a broader, narrativewide perspective? For example, when writing a story, do they recall events from earlier chapters or rely mostly on recent developments? While difficult to study these questions rigorously in humans, large language models (LLMs) offer a tractable experimental analogue. This leads us to ask: How far back must a model look to predict the next token accurately? Although modern transformerbased LLMs can attend to thousands of tokens (Beltagy et al., 2020; Dai et al., 2019), it remains unclear and unquantified how often that capacity is used at inference time, and how often predictions depend on distant information or primarily on local spans.

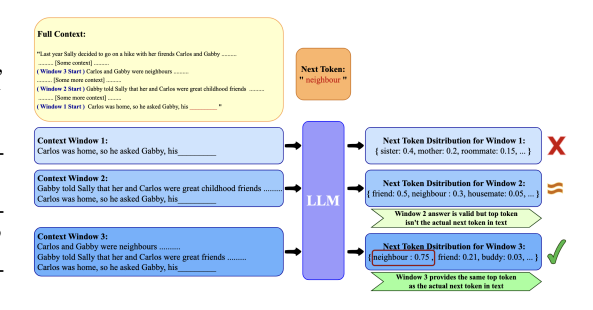


Figure 1: Short-context dominance hypothesis. In this example, with context 1 the model fails to predict the ground-truth "neighbour," Context 2 produces a semantically valid alternative "friend," and when using Context 3, the model correctly predicts "neighbour." Our work (1) systematically validates the hypothesis, (2) develops methods to detect when longer context is truly needed, and (3) leverages these insights to improve language model sampling by correcting short-context bias.

We posit the *short-context dominance hypothesis*: for the majority of natural-language sequences, the information required to accurately predict a valid next token is contained within a *short*, *local* prefix of length $k \ll n$, where n is the full-context length of the sequence. Confirming this hypothesis could: (1) reveal how much model capacity is truly needed for next-token prediction of a given sequence, (2) inform the design of better performing sampling methods, and, eventually, (3) identify opportunities for architectural or training modifications that leverage locality for computational efficiency.

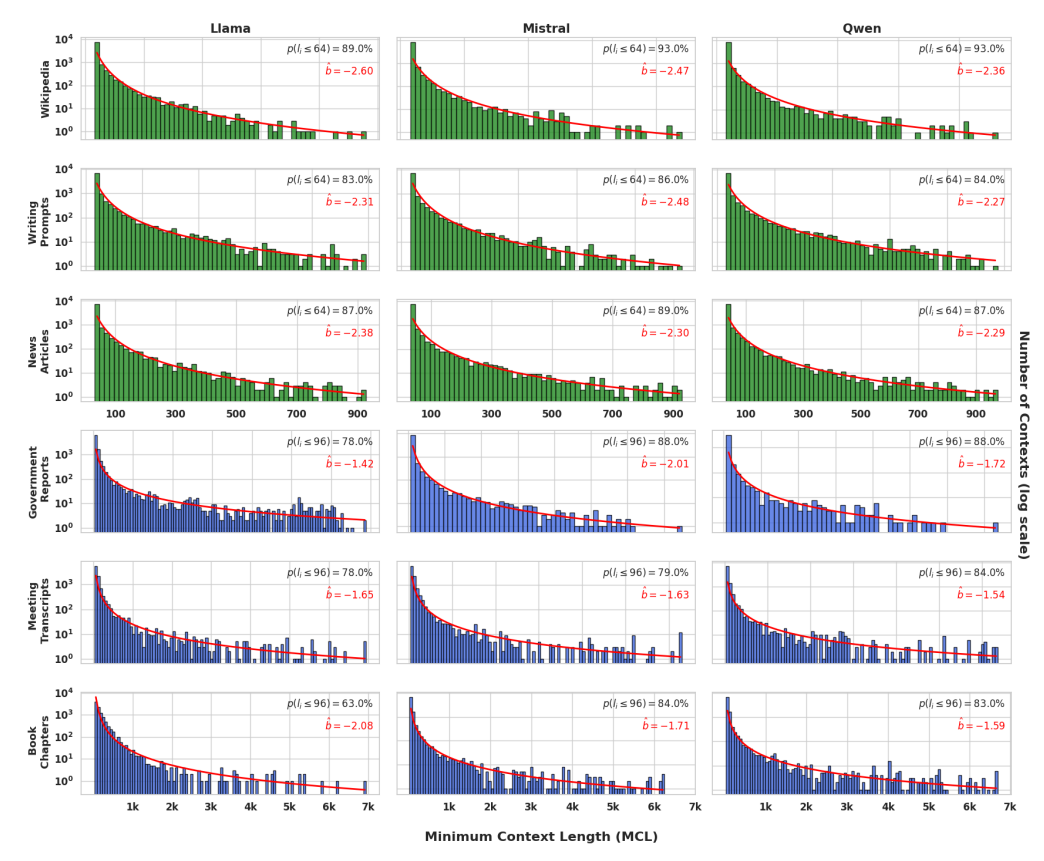


Figure 2: **Distribution of MCL:** Minimum context window needed to confidently predict the next token across sampled sequences, six datasets, and three LLMs. \hat{b} denotes the slope of the log-log fit. Blue/green distinguishes between long (\geq 6k tokens) and short (\geq 1k tokens) documents, respectively.

Measuring natural-language local context dependency. To test our hypothesis, we introduce Minimal Context Length (MCL), which quantifies how much local context suffices for a language model, used as oracle, to confidently predict the ground-truth next token of a sequence. We sample sequences of varying lengths from various sources and filter for cases where an LLM confidently predicts the actual next token in the corpus, aiming to mitigate confounding effects of LLM limitations. To quantify MCL, we iteratively increase the prefix length of each sequence until the model confidently outputs the ground-truth next token. We find consistently that 75-80% of sequences with lengths 100-7k tokens rely on at most 32-96 last tokens, supporting our hypothesis. See Fig. 2.

Practical long-context detection. We develop a practical variant of MCL, the **Distributionally Aware Minimum Context Length (DaMCL)**, that does *not* require ground-truth knowledge and is compatible with sampling strategies beyond greedy decoding. We validate that DaMCL remains consistent with the short-context dominance hypothesis. Importantly, we show that it enables accurate classification of sequences as *short-context* (where a 32-token prefix suffices) or *long-context* (requiring longer context). Since detection operates without ground-truth information, it is practical for inference-time applications.

Post-hoc short-context dominance correction. With a long-context detector at hand, we finally test a hypothesis that short-context dominance induces a corresponding bias in LLMs themselves: Since sequences predominantly require only short context, models are implicitly trained on distributions heavily skewed toward local dependencies, biasing them toward common completions and filler words predictable from short local context, hurting prediction for long-context sequences (Sharma et al., 2023; Malkin et al., 2022; Duh et al., 2024). We validate such a short-context bias by applying TaBoo (**Targeted Boo**sting), an intuitive decoding algorithm that counteracts the skew: for sequences that we detect as being long-context, TaBoo identifies and boosts tokens that are long-context-relevant. On Q&A datasets with inherent long-context dependencies, TaBoo consistently outperforms vanilla nucleus sampling and competitive logit-adjustment methods across model architectures.

2 RELATED WORK

We summarize the most closely related works below and defer detailed discussion to Appx. B.

Long context utilization analysis. Prior studies demonstrate that LMs often underutilize available context (Khandelwal et al., 2018; Sun et al., 2021; Liu et al., 2023). These findings have inspired algorithmic interventions at both system and data levels (Zhang et al., 2024; Borgeaud et al., 2022; Izacard et al., 2022; Chen et al., 2025; Chuang et al., 2025). A more closely related recent study by Fang et al. (2025) provides methodology for detecting tokens with long context relevance and emphasizing them upon evaluation and fine-tuning. Our work differs by providing systematic quantification of minimal context requirements from the perspective of natural language properties themselves, introducing practical detection methods that operate without ground-truth tokens (a key distinction to Fang et al. (2025)), and demonstrating targeted inference-time interventions.

Contrastive decoding. Several inference-time methods address hallucination in long-context generation through contrastive approaches (Li et al., 2023; Zhao et al., 2024; Liu et al., 2021). Building on (Li et al., 2016; Brown et al., 2020), Malkin et al. (2022); Duh et al. (2024) reweight distributions by contrasting long vs. short contexts. CAD (Duh et al., 2024) is most closely related to our TaBoo algorithm, but differs fundamentally in both motivation and implementation. While CAD uniformly adjusts output probabilities for all sequences and tokens through contrastive considerations, our algorithm stems from the short-context dominance hypothesis and applies targeted adjustments to long-context sequences and their long-range-relevant tokens. van der Poel et al. (2022) apply entropy-based selection for contrastive decoding, but their method differs again in both theoretical motivation and technical implementation. Beyond distinctions specific to TaBoo, we systematically study minimal context length requirements in natural language and our long-context detection methods could apply beyond inference-time correction.

n-gram models. Recent work has revisited n-gram models as complements to neural language models (Li et al., 2022; Liu et al., 2025; Nguyen, 2024). The success of such inherently short-range models (even Liu et al. (2025)'s Infini-gram typically captures at most 32-token dependencies) provides indirect evidence toward short-context dominance in natural language. Our systematic quantification of minimal context requirements offers a principled explanation of this, supporting the broader thesis that majority of language understanding tasks require primarily local information.

3 LEAST CONTEXT FOR PREDICTION

In this section, we answer the following question: For a given randomly sampled context and next-token, what is the minimum sub-context needed to predict the actual next token correctly?

3.1 MINIMAL CONTEXT LENGTH

We isolate sequences s for which the LLM, using greedy decoding, **correctly** and **confidently** predicts the actual next token t in the corpus. By focusing on these high-quality predictions, we approximate using the LLM as a statistical oracle to study context dependency. We define MCL as follows.

Definition 1. The *Minimal Context Length* (MCL) of sequence s given its next token t is the length ℓ of the shortest prefix $s_{[-\ell]}$ so that the model output given the prefix is correct and confident. Formally,

$$\mathsf{MCL}\left(\mathbf{s}|t\right) := \arg\min_{l \in |\mathbf{s}|} \left\{ l \mid \mathsf{Top}_{1}(\mathbf{s}_{[-l:]}) = t, \ \Delta\mathsf{Conf}(\mathbf{s}_{[-l:]}) \geq \delta \right\} \tag{1}$$

Here, $\mathbf{s}_{[-\ell:]}$ denotes the prefix of the last ℓ tokens of sequence \mathbf{s} of length $|\mathbf{s}|$; $\mathsf{Top}_1(\cdot)$ returns the token with highest model output probability given the input sequence; and $\Delta\mathsf{Conf}(\cdot)$ returns the gap in probability between the top-ranked and second-best token, which must exceed confidence threshold $\delta \in [0,1]$. For concreteness in our experiments, we set $\delta = 0.2$ (see Appx. C.1 for ablation). By definition, a larger MCL implies that the model requires information from earlier in the context to predict the next token correctly, while smaller MCL indicates greater reliance on local context.

3.2 EXPERIMENTAL SETUP

Datasets. We experiment on the following natural-language documents. Short documents: Reddit Writing Prompts (Fan et al., 2018), CNN/DailyMail News Articles (Hermann et al., 2015; Nallapati

et al., 2016) and *Wikipedia* articles from WikiText-103 (Merity et al., 2016). Long documents: U.S. *Government Reports* from GovReport (Huang et al., 2021), *Meeting Transcripts* from QMSum Zhong et al. (2021) and story *Book Chapters* BookSum (Kryściński et al., 2022). These appear in the LongBench and LongEval (Bai et al., 2024; Krishna et al., 2023) benchmarks and are believed to have inherent long-context qualities. We further experiment with documents of different languages using (Schwenk et al., 2019). Datasets are deliberately chosen for their natural-language nature and general domain coverage, avoiding specialized formats (mathematics/code), which may exhibit different context dependencies. We leave such extensions to future work.

LLM Oracles. We evaluate three open-weight models: LLaMA-3-8B (Grattafiori et al., 2024), Mistral-7B-Instruct (v0.2) (Jiang et al., 2023) and Qwen2-7B (Yang et al., 2024). We assume that these models are sufficiently capable to exhibit reliable performance on next-token prediction and question answering tasks. Recall also that we isolate sequences that the models confidently predict the next token. All experiments are performed on a V100 Nvidia GPU with 32GB of memory.

Choice of sequences. We form sequences s by parsing documents from the datasets. For short documents we sample 100 unique documents of length at least 1k and only keep their first 1k tokens. For long documents we sample documents of lengths $n \in [6,7]k$, in order to focus our analysis on long-context inputs. We sample 100 sequences s and their ground-truth next-token t from each document. We filter for sequences with correct and confident predictions. We also make sure to avoid biases toward either shorter or longer sequences. Concretely, for our 1k token length windows (0-1k for regular documents and 6-7k for long context data), we ensure to sample the same number of sequences from sizes $[32,100], [100,200], \cdots, [900,1000]$. Overall, this yields 10k unique sequences (100 sequences \times 100 documents) and their respective next tokens for each dataset.

MCL Algorithm. To determine the MCL as per Defn. 1, we evaluate a model's predictions using increasing prefix sizes $l \in \{32, 48, 64, \ldots, |\mathbf{s}|\}$, starting from 32 tokens and incrementing by 16. For the longer documents, we start from 32 and increment by 64. Starting from 32 tokens is motivated by prior work suggesting this length captures local context beyond classical n-gram statistics (Malkin et al., 2022; Liu et al., 2025; Fang et al., 2025). For each window size, we evaluate the model's output distribution and stop once it confidently predicts the ground-truth next token. In practice, we provide the full input to preserve positional encoding and simulate truncated contexts via attention masking.

3.3 RESULTS AND DISCUSSION

Fig. 2 shows that the distribution of MCL $(\mathbf{s}|t)$ as defined in Equation 1 is highly skewed (note the histogram y-axis in log scale), indicating that the model requires only the last 32-96 tokens for the majority of contexts (~ 80 –90%) to confidently predict the next token (MCL $(\mathbf{s}|t) \leq 32$ or 96). This observation formally confirms that for majority of queries, the LLM only needs highly localized information from the context to correctly and confidently predict the token.

To quantify short-context reliance at finer granularity, we examine the power-law exponent \hat{b} by fitting $y=a\cdot x^{-b}$ in log-log space. For shorter documents, we observe values of $\hat{b}\in[-2.5,-2]$, and for longer documents, \hat{b} falls in the range [-2,-1.5]. Both ranges indicate strong power-law decay, demonstrating short-context sufficiency even in inherently long-context datasets such as *Government Reports, Meeting Transcripts*, and *Book Chapters*. We further validate these findings across linguistic and domain variations through experiments detailed in Appx. C.2. Table 3 demonstrates that this pattern holds consistently: **Short-context dominance persists across our experimental setups**.

Validating the short-context dominance hypothesis carries implications for both pretraining and evaluation: Since most predictions require only highly localized information, then standard training objectives and perplexity-based evaluations are inherently skewed toward short-range dependencies, potentially obscuring true progress on long-context reasoning. This helps explain prior findings that only small fraction of tokens benefit from contexts larger than 2K (Sun et al., 2021). It also reinforces recent critiques (Fang et al., 2025) that token-level perplexity is an insufficient metric for long-context evaluation—even on datasets with genuine long context dependencies, such as *Government Reports*.

4 DISTRIBUTIONAL AWARENESS

MCL evaluates whether the ground-truth next token from the dataset can be predicted with a shorter prefix. Intuitively, natural language often permits multiple valid next tokens, and models may assign high probability to plausible alternatives that differ from the ground-truth token in the dataset.

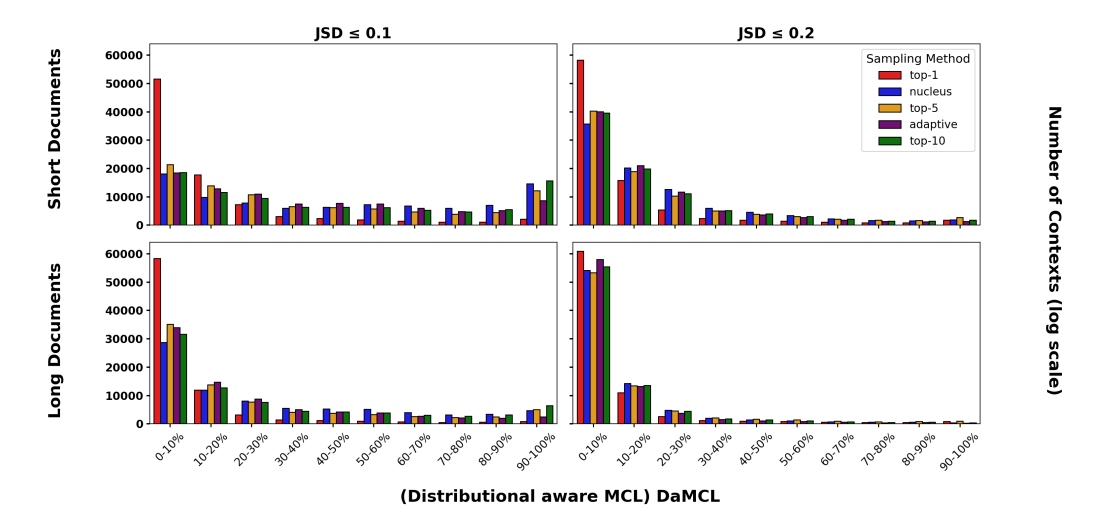


Figure 3: Distribution of DaMCL: DaMCL measurements for various sampling strategies and relative thresholds. Results are shown separately for short- (top row) and long- (bottom row) documents to highlight potential differences in behavior. While the overall trend resembles the heavytailed decaying pattern observed in standard MCL (see Fig. 2), the choice of threshold influences the outcome. Each subplot reflects results aggregated over all model-dataset combinations, as only minor deviations were observed across different configurations under identical hyperparameters.

Definition 1 is also limited to greedy decoding, while popular natural language generation methods often rely on sampling strategies that draw from multiple probable tokens (Holtzman et al., 2020; Basu et al., 2021; Zhu et al., 2024). These considerations (see also Appx. D.1) motivate us to introduce here a more flexible MCL formulation.

DISTRIBUTION AWARE MCL

Consider decoding strategy ϕ that modifies the model's raw probability distribution. For example, nucleus sampling Holtzman et al. (2020) selects a subset of tokens whose cumulative probability mass reaches threshold p (e.g. p = 0.9), then produces a renormalized distribution $\mathbf{p}_{\phi}(\mathbf{s})$ with support on this subset and zero probability to tokens otherwise. More generally, our framework accommodates any decoding strategy ϕ that produces a probability distribution $\mathbf{p}_{\phi}(\mathbf{s})$. We introduce DaMCL to find the smallest prefix $\mathbf{s}_{[-\ell:]}$ such that $\mathbf{p}_{\phi}(\mathbf{s}_{[-\ell:]})$ is sufficiently similar to $\mathbf{p}_{\phi}(\mathbf{s})$.

Definition 2. The **Distribution-aware Minimal Context Length** (DaMCL) of a sequence s, given decoding strategy ϕ , a probability-similarity metric \mathcal{M} , and a similarity threshold ϵ , is defined as the length of the shortest prefix for which the decoding-based next-token distribution given the prefix $\mathbf{p}_{\phi}(\mathbf{s}_{[-\ell:]})$ lies within an ϵ -neighborhood of the full-context distribution $\mathbf{p}_{\phi}(\mathbf{s})$. Formally, we define: $\mathsf{DaMCL}_{\phi}^{\mathcal{M}}(\mathbf{s}, \epsilon) := \arg\min_{l \in [\mathbf{s}]} \left\{ l \mid \mathcal{M}(\mathbf{p}_{\phi}(\mathbf{s}_{[-l:]}); \mathbf{p}_{\phi}(\mathbf{s})) \leq \epsilon \right\}.$

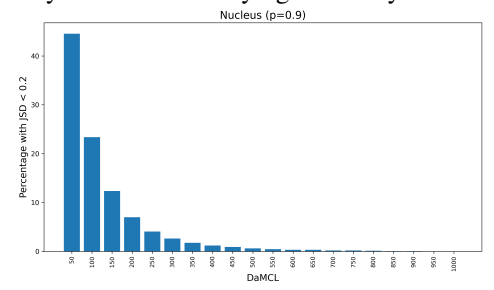
$$\mathsf{DaMCL}_{\phi}^{\mathcal{M}}\left(\mathbf{s}, \epsilon\right) := \arg\min_{l \in |\mathbf{s}|} \left\{ l \mid \mathcal{M}(\mathbf{p}_{\phi}(\mathbf{s}_{[-l:]}); \, \mathbf{p}_{\phi}(\mathbf{s})) \leq \epsilon \right\}$$

While this definition accommodates any distance metric \mathcal{M} , we specifically use the Jensen-Shannon Distance (JSD) throughout our experiments. For distributions p_1 , p_2 in the $|\mathcal{V}|$ -dimensional simplex, JSD is defined as $JSD(\mathbf{p}_1\,;\,\mathbf{p}_2):=\sqrt{\frac{1}{2}}KL(\mathbf{p}_1\|\mathbf{q})+\frac{1}{2}KL(\mathbf{p}_2\|\mathbf{q})$, where $\mathbf{q}:=\frac{1}{2}(\mathbf{p}_1+\mathbf{p}_2)$, and $\mathrm{KL}(\mathbf{p}_1\|\mathbf{p}_2) := \sum_{t \in \mathcal{V}} [\mathbf{p}_1]_t \log \frac{[\mathbf{p}_1]_t}{[\mathbf{p}_2]_t}$ is the Kullback-Leibler divergence. We choose JSD because it is a proper distance metric satisfying the triangle inequality and is widely employed in knowledge distillation Gu et al. (2024) and language model evaluation Ji et al. (2023a). The above definition of DaMCL (1) relies on measuring the difference between distributions as opposed to a single token, and, (2) does not require ground-truth information regarding the actual next token of sequence s.

4.2 EXPERIMENTAL SETUP

DaMCL evaluation. We evaluate DaMCL over several decoding strategies: Top-K sampling (K=1 for greedy) with $K \in [10]$ (Radford et al., 2019; Fan et al., 2018), nucleus sampling with p=0.9 (Holtzman et al., 2020), and adaptive sampling with ϵ =0.001 (Zhu et al., 2024). We evaluate two threshold values JSD \leq 0.1 and JSD \leq 0.2 to study the effect of varying similarity criteria.

Lower thresholds correspond to stricter conditions for accepting a local prefix as equivalent to the full context. Complementary to the setup of Sec. 3.3, we use lengths ℓ of prefixes based on percentiles of the full sequence (specifically, the last 10% to 100%) rather than fixed-length truncation. The length |s| of the full sequences is restricted to [6, 7]k for long docs and [200, 1000] otherwise.



4.3 RESULTS AND DISCUSSION

To begin with, Fig. 3 for JSD ≤ 0.2 reveals a similar bias toward short context as with MCL. Yet, note that the drop in DaMCL is not as dramatic as observed

Figure 4: DaMCL distribution for nucleus sampling with fixed sub-context increments. Still heavily biased towards short context.

when using MCL suggesting that, from a distributional standpoint, larger portions of context are required to ensure similarity compared to the ground-truth-token-based MCL.

When enforcing stricter similarity requirements (JSD \leq 0.1) we find the distribution becomes flatter and even experiences a U-shaped structure. This suggests that a larger subset of tokens either resolve with short contexts or require nearly the full input to reach distributional convergence. We further analyze this in Appx. D.3 and discover that this bimodality is mainly attributed to the shorter sequences. Indeed, we find that the long documents, for which all sequences have more than 6k tokens, do not experience the bimodality to the same degree.

Further, while all decoding strategies show a similar long-tailed behavior for $JSD \leq 0.2$, for the more strict conditions their DaMCL flatness differs. While top-1 sampling continues to exhibit standard decay across settings, broader sampling methods such as nucleus, top-5, top-10, and adaptive sampling increasingly lead to flatter distribution. As these methods spread probability mass across a wider support set, the resulting distributions become smoother and more diffuse, making convergence under tight JSD thresholds more difficult.

For completeness, we also provide results for fixed sub-context lengths in Fig. 4, where we use fixed increments of 50 (for efficiency). These results suggest that short context bias still remains even when using distribution shift as the metric for detecting minimal context length, even if the severity is somewhat reduced compared to greedy decoding from MCL. Further results are in Appx. D.3.

5 Long-Context Sequence Detection

We have seen that for the majority of sequences a valid next-token can be generated with access to only a short local prefix. Specifically, in Sec. 4, to avoid the need for knowing the actual next-token of a sequence, we introduced the idea of quantifying whether a prefix is a good proxy of the full-context by evaluating the JSD of the respective model output probabilities. Here, we build on these insights to develop a long-context detector that can distinguish between *short-context sequences*, where a short prefix of fixed length suffices, and *long-context sequences*, which require longer context information.

5.1 DISTRIBUTIONAL-AWARE LONG-CONTEXT SEQUENCE DETECTION

To develop our long-context detector, we first define the following metric.

Definition 3. The **Long-Short Distribution Shift (LSDS)** of sequence \mathbf{s} is the JSD between the next-token distributions obtained with decoding strategy ϕ when given a short prefix of length 32 versus the full context. Formally, LSDS $(\mathbf{s}) = JSD(\mathbf{p}_{\phi}(\mathbf{s}_{[-32:]}), \mathbf{p}_{\phi}(\mathbf{s}))$.

For concreteness, unless otherwise stated, we fix ϕ to nucleus sampling with parameter p=0.9 (Holtzman et al., 2020). (Ablation results on different metrics and p values in Appx E.2.) Finally, we fix the prefix length to 32 based on our findings in Sec . 3 and consistent with Liu et al. (2025).

Controlled validation. To demonstrate that LSDS can effectively detect long-context sequences, we conduct a controlled needle-in-a-haystack experiment adapted from Kamradt (2023). We create

325

326

327

328

330

331

332

333

334

335

336 337 338

340 341

342

343

344

345

346

347

348

349

350

351

352

353

354

355

356

357

358

359

360

361 362

364

366 367

368

369

370

371

372

373

374

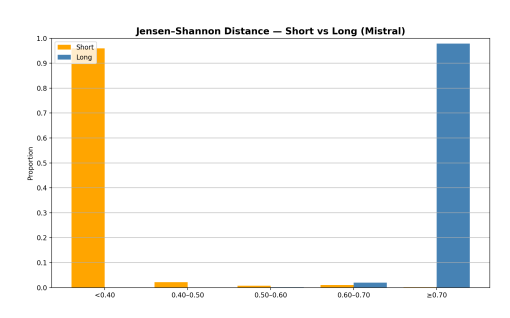
375

376

377

short and long queries, such that only in the former the answer appears in the final 32 tokens; see Appx. E.1.1 for details and example illustration. Figure 5 shows the resulting LSDS distributions for Mistral-7B-Instruct (v0.2). We observe a clear separation between categories despite no ground-truth next-token information: short-context sequences concentrate at low LSDS values (≤ 0.4), while long-context sequences dominate high LSDS values (≥ 0.7). Similar patterns hold for LLaMA-3-8B/Qwen2-7B (see Appx. E.1.1).

Long-context detector. Based on these findings, we define our long-context detector as a simple thresholding classifier: LSDS $(\mathbf{s}) \geqslant_{\mathrm{short}}^{\mathrm{long}} \tau$ where τ is a threshold determined from validation data or prefixed. In the following sections, we analyze the behavior of the detector on natural text.



5.2 EVALUATION ON NATURAL TEXT

Figure 5: Distribution of LSDS (s) values for short- and long-context sequences for Mistral-7B-Instruct on controlled validation setup.

In natural text, determining the true context dependency requires an oracle with access to the actual next token. We employ two such oracles to establish

ground-truth short-context vs long-context labels for sequences. (1) MCL Oracle: For s with nexttoken t, we classify s as long-context iff MCL (s|t) ≥ 32 (see Defn. 1). (2) LSD Oracle: Following Fang et al. (2025), we classify s as long-context iff LSD(s|t) > 2 & $LCL(s|t) \ge -1$ (details in Appx. E.1.3). Both oracles require knowledge of ground-truth next token and thus cannot be deployed at inference time. We show that LSDS-based classification agrees well with these oracles despite not knowing the ground-truth.

Results. Figure 6 demonstrates strong agreement between LSDS and the LSD Oracle across Government Reports and Reddit Writing Prompts datasets. Using $\tau = 0.6$, we find consistently 80 - 90% of oraclelabeled long-context sequences being classified by LSDS as long-context, while fewer than 5-10% of short-context sequences are mislabeled. This pattern holds consistently across LLaMA-3-8B/Mistral-7B-Instruct/Qwen-2-7B and both oracles (Appx. E.1), verifying LSDS as a reliable proxy for short vs long context detection.

Threshold robustness. Through extensive ablations deferred to Appx. E.1, we find that threshold choices are robust across models and datasets. While a fixed threshold works well generally, task-specific tuning can optimize precision-recall trade-offs.

Ablation on short-context length. We test prefixeslengths $\{8, 16, 32, 64\}$ on Mistral-7B-Instruct-v0.2 (GovReport). Consistent with intuition, too short prefixes (8, 16) lead to larger overlap between short/long distributions, while our chosen values (32, 64) show clearer separation with fewer false positives. We also show good performance particularly with respect to consistency among datasets when adaptively setting the context length to $0.1|\mathbf{s}|$. See Appx. E.3.

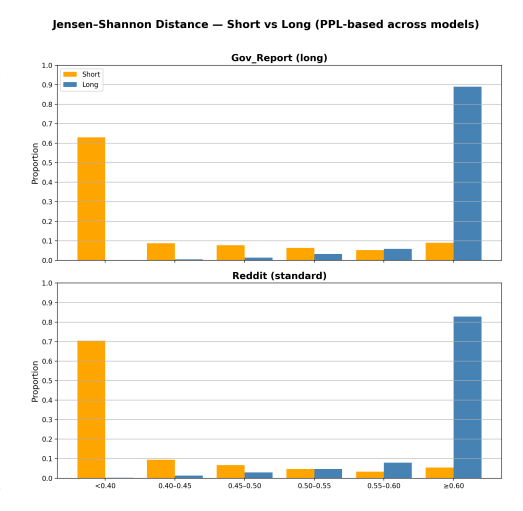


Figure 6: Distribution of LSDS (s) for shortand long-contexts on 2 GovReport (long doc) and Reddit Writing Prompts (short doc), pooled across three models. Illustrates a clear distinction between long and short contexts.

Computational overhead. LSDS requires one extra short forward plus JSD calculation beyond normal generation. On Qwen2.5-1.5/7/14B, this adds 35-67 ms across sizes, which is negligible at long contexts, e.g. $\approx 6 - 8\%$ at $|\mathbf{s}| = 6000$. See Appx. E.4.

6 Long-Context Token Boosting

Fewer exposures to long-context sequences may creates a potential bias toward completions that follow from local context, overshadowing long-range dependencies. Can we identify tokens in the vocabulary that are more relevant to full-context information rather than local context?

If so, we could favor generating such tokens when we detect a sequence requires long-context reasoning (which, as shown in the previous section, we can reliably identify). Here, we show this is possible and evaluate our method on text-based question answering, a standard benchmark for assessing long-context reasoning capabilities (Liu et al., 2023; Krishna et al., 2023; Beltagy et al., 2020; Bai et al., 2024).

Figure 7: An example illustrating how a shift in the model's next token probabilities when given the long vs short context could help us recognizing the more relevant tokens. Here, boosting the probability of said tokens leads to a more accurate next token distribution.

6.1 IDENTIFYING LONG-CONTEXT-RELEVANT TOKENS

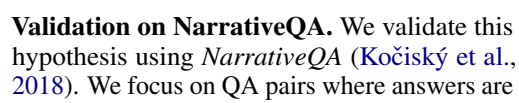
First, we show how to identify tokens that are more relevant to full-context information than to local context. Consistent with our theme, the insight is that tokens requiring long-range dependencies should exhibit larger probability increases when given access to full versus short context.

Definition 4. The Long-Short Probability Shift (LSPS) of a vocabulary token t given sequence s is defined as the change in the assigned probability moving from short to full context under decoding ϕ :

$$\mathsf{LSPS}\left(t|\mathbf{s}\right) = \left[\mathbf{p}_{\phi}(\mathbf{s})\right]_{t} - \left[\mathbf{p}_{\phi}(\mathbf{s}_{[-32:]})\right]_{t} \,.$$

Here, for probability vector \mathbf{p} , $[\mathbf{p}]_t$ denotes its t-th entry. As in the previous section, we fix the prefix length to 32 and, unless otherwise stated, for ϕ , we use nucleus sampling (p = 0.9).

Our hypothesis is that tokens genuinely requiring long-context information will show positive LSPS values, as their relevance becomes apparent only with access to the complete context. Conversely, tokens predictable from local context should show small or (even) negative shifts.



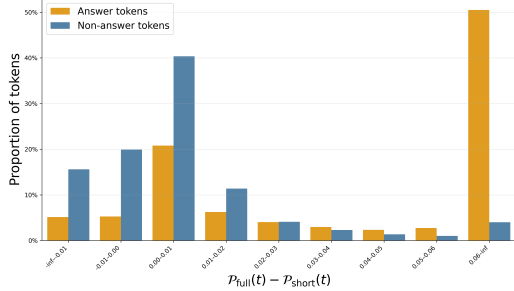


Figure 8: An example showing how a shift in the long- vs. short-context next-token distribution can signal most long-context-relevant tokens.

1–2 words (typically character names or locations), filtering out cases resolvable without the story context. Given a context with the story, question, and partial answer, we classify the ground-truth next token as an *Answer Token* and all other vocabulary tokens as *Non-Answer Tokens*. Figure 8 shows LSPS distributions for both categories using LLaMA-3-8B.

Observe the clear separation: Answer tokens exhibit significantly higher LSPS values, confirming that long-context relevant tokens can be identified through their probability shifts. Concretely, using threshold $\epsilon \in [0.05, 0.07]$, we capture over 50% of answer tokens while maintaining low false positive rates (< 5%) on non-answer tokens. Our objective is capturing long-context-relevant tokens while avoiding irrelevant ones, which this approach achieves effectively. In Appx. F, we compare our method to a modified version that uses log-probability ratio (rather than difference) common in prior work (Duh et al., 2024; Malkin et al., 2022; van der Poel et al., 2022; Fang et al., 2025), demonstrating the superior stability and precision of our difference-based approach.

6.2 TARGETED LONG-CONTEXT TOKEN BOOSTING

Knowing how to (1) detect long-context sequences using LSDS and (2) identify long-context relevant tokens via LSPS, we now combine these tools to improve Q&A performance. The core insight is to

Table 1: F1, BLEU, and ROUGE-L (Average over all generations and Best-per-example in parentheses). Bold = best Average, Underline = best Best-per-example. We omit results for LLaMA-2-7B on MultifieldQA-en because its context window (4,096 tokens) is insufficient to process the long input passages in this dataset. We include the standard errors (SE) in Appx. F Table 9 for reference.

Model	Method	NarrativeQA			HotpotQA			MultifieldQA-en		
		F1(†)	BLEU(↑)	ROUGE-L(↑)	F1(↑)	BLEU(↑)	ROUGE-L(↑)	F1(↑)	BLEU(↑)	ROUGE-L(↑)
LLaMA-2-7B	Vanilla	16.1 (36.8)	2.9 (8.3)	22.4 (46.2)	25.2 (51.8)	7.7 (17.0)	32.5 (61.0)	NA	NA	NA
	CAD	22.5 (43.3)	4.3 (9.7)	30.7 (51.6)	28.3 (53.1)	8.5 (16.7)	34.3 (59.8)	NA	NA	NA
	TaBoo	24.1 (<u>44.9</u>)	4.9 (10.9)	31.7 (<u>53.5</u>)	32.8 (<u>56.4</u>)	10.3 (<u>18.7</u>)	39.6 (<u>63.3</u>)	NA	NA	NA
LLaMA-3-8B	Vanilla	24.0 (48.8)	4.9 (12.1)	32.7 (57.9)	29.2 (<u>56.3</u>)	9.0 (18.8)	41.6 (68.6)	19.9 (<u>35.7</u>)	7.7 (16.6)	24.0 (41.1)
	CAD	35.4 (<u>55.3</u>)	7.3 (13.5)	49.4 (<u>63.5</u>)	27.7 (46.6)	8.5 (14.7)	46.9 (65.3)	18.8 (<u>33.8</u>)	6.4 (13.8)	26.2 (43.1)
	TaBoo	32.0 (53.5)	7.2 (<u>14.7</u>)	42.3 (62.8)	33.1 (55.6)	10.6 (<u>19.1</u>)	48.1 (<u>69.6</u>)	21.9 (<u>35.4</u>)	9.1 (18.2)	28.2 (<u>44.0</u>)
Mistral-7B-v0.1	Vanilla	25.7 (49.7)	5.1 (12.2)	33.7 (58.4)	33.0 (<u>60.1</u>)	10.1 (<u>19.8</u>)	43.1 (<u>69.2</u>)	20.6 (33.6)	6.9 (14.2)	26.0 (41.3)
	CAD	34.3 (53.4)	7.1 (13.6)	43.1 (62.7)	35.9 (58.7)	11.0 (18.8)	41.6 (<u>64.3</u>)	18.8 (32.7)	5.9 (12.8)	24.9 (41.8)
	TaBoo	35.3 (<u>55.2</u>)	7.7 (<u>15.0</u>)	44.4 (<u>64.6</u>)	37.1 (59.3)	11.7 (19.7)	46.3 (<u>67.5</u>)	23.0 (37.0)	8.6 (<u>16.3</u>)	29.5 (<u>45.3</u>)
Qwen2-7B	Vanilla	33.6 (53.1)	8.1 (14.8)	42.4 (62.9)	59.4 (<u>80.5</u>)	20.1 (<u>29.0</u>)	62.9 (<u>82.7</u>)	31.1 (44.9)	15.1 (<u>25.9</u>)	41.3 (<u>59.7</u>)
	CAD	36.6 (50.2)	8.8 (13.6)	45.3 (59.9)	59.3 (75.6)	20.5 (27.4)	62.2 (78.1)	30.6 (43.8)	14.0 (23.5)	40.0 (55.3)
	TaBoo	38.5 (<u>53.6</u>)	9.7 (<u>15.4</u>)	48.2 (<u>63.6</u>)	63.2 (79.2)	21.7 (28.4)	66.6 (81.6)	32.3 (45.3)	15.3 (4.7)	42.3 (58.8)

promote those identified long-context relevant tokens, downplaying biases from the short context. Simultaneously, this can help downplaying tokens that are assigned high probability as an artifact of noise (Sharma et al., 2023), biases rooted in training data due to potential word/token imbalances (Razeghi et al., 2022; Kassner et al., 2020) and hallucination (Ji et al., 2023b).

TaBoo (**Targetted**) **Boosting.** Our algorithm TaBoo modifies the probability distribution as per the above intuition. Algorithm 1 details the complete procedure: (1) Detect long-context sequences using LSDS with threshold γ , (2) Identify long-context relevant tokens where LSPS $\geq \epsilon$, and (3) boost their probabilities by factor λ before renormalization and nucleus sampling. See Algorithm 9 in Appx. F.

Experimental setup. We evaluate on NarrativeQA (Kočiský et al., 2018), HotpotQA (Yang et al., 2018), and MultiFieldQA (Bai et al., 2024) from the LonBench dataset. Focusing on stories with \geq 1000 tokens to emphasize long-context dependencies, we sample 3,000 examples from NarrativeQA and HotpotQA while using the full 150 examples from MultiFieldQA. We set $\gamma=0.1225^1$ and $\epsilon=0.05$. We test on LLaMA-2-7B, LLaMA-3-8B, Mistral-7B, and Qwen-2-7B. For each question-text pair, we generate 5 answers using nucleus sampling and report both average and best-of-5 F1/BLEU/ROUGE scores. We compare our TaBoo approach against two baselines: (1) vanilla nucleus sampling, and (2) Context Aware Decoding (CAD) (Malkin et al., 2022; Duh et al., 2024) with $\alpha=0.5$, which applies probability adjustments to all generations and their tokens, unlike our targeted boosting of only long-context relevant tokens in detected long-context sequences.

Results. Table 1 shows TaBoo consistently outperforms vanilla nucleus sampling across all models and datasets. Compared to CAD, TaBoo achieves superior F1 performance on 11 out of 12 dataset-model combinations, losing only on NarrativeQA with LLaMA-3-8B (although not wrt BLEU score). The improvements generalize across different model architectures and scale to higher-performing base models like Qwen2-7B. Best-per-example scores also favor TaBoo, with improvements over vanilla ranging from 0.5-8.1 F1 points and generally outperforming CAD as well. Additional results in Appx. F.1, F.3 present ablations on hyperparameter selection $(\gamma, \epsilon, \lambda)$. Experiments for short summarization on XSUM (Narayan et al., 2018) are also deferred to Tab. 7 in the appendix, where we also discuss the computational overhead of LSDS (thus, also TaBoo) are minimal for long sequences.

7 Outlook

Our work provides a systematic framework for understanding context dependency in language models, with implications for inference efficiency in tasks like QA through principled post-hoc decoding. Specifically, our ability to detect long-context requirements without ground-truth tokens opens opportunities for context-aware generation methods, but also for more targeted evaluation of long-context capabilities and improved training approaches (e.g., following Fang et al. (2025)). Beyond immediate applications, our findings reveal the short-context dominance hypothesis as an inherent property of natural language sequences, with potential broader implications for understanding how language models process and generate text, such as providing alternative motivations for recently proposed logit-adjusted decoding modifications in the hallucination literature Duh et al. (2024).

¹The boosting threshold $\gamma=0.1225$ is intentionally more liberal than the classification threshold $\tau=0.6$ used in Sec. 5. While τ was set conservatively for clear evaluation of long vs. short context, γ captures borderline cases where targeted boosting may still be beneficial.

8 REPRODUCIBILITY STATEMENT

Following reproducibility requirements, we have ensured to include all detail regarding experimental setup in the text. Regarding the implementation of comparable methods or baseline, we have followed the source reference and common practice to the best of our abilities. Additionally, we have python files and notebooks to recreate versions of our experiments on MCL, long-context detection and the implementation of our TaBoo algorithm.

REFERENCES

- Yushi Bai, Xin Lv, Jiajie Zhang, Hongchang Lyu, Jiankai Tang, Zhidian Huang, Zhengxiao Du, Xiao Liu, Aohan Zeng, Lei Hou, Yuxiao Dong, Jie Tang, and Juanzi Li. Longbench: A bilingual, multitask benchmark for long context understanding, 2024. URL https://arxiv.org/abs/2308.14508.
- Sourya Basu, Govardana Sachitanandam Ramachandran, Nitish Shirish Keskar, and Lav R. Varshney. Mirostat: A neural text decoding algorithm that directly controls perplexity, 2021. URL https://arxiv.org/abs/2007.14966.
- Iz Beltagy, Matthew E. Peters, and Arman Cohan. Longformer: The long-document transformer, 2020. URL https://arxiv.org/abs/2004.05150.
- Yoshua Bengio, Réjean Ducharme, Pascal Vincent, and Christian Jauvin. A neural probabilistic language model. *Journal of Machine Learning Research*, 3:1137–1155, 2003.
- Sebastian Borgeaud, Arthur Mensch, Jordan Hoffmann, Trevor Cai, Eliza Rutherford, and et al. Katie Millican. Improving language models by retrieving from trillions of tokens, 2022. URL https://arxiv.org/abs/2112.04426.
- Tom B Brown, Benjamin Mann, Nick Ryder, Melanie Subbiah, Jared Kaplan, Prafulla Dhariwal, Arvind Neelakantan, Pranav Shyam, Girish Sastry, Amanda Askell, et al. Language models are few-shot learners. In *Advances in Neural Information Processing Systems*, volume 33, pp. 1877–1901, 2020.
- Jianghao Chen, Junhong Wu, Yangyifan Xu, and Jiajun Zhang. Ladm: Long-context training data selection with attention-based dependency measurement for llms, 2025. URL https://arxiv.org/abs/2503.02502.
- Shouyuan Chen, Sherman Wong, Liangjian Chen, and Yuandong Tian. Extending context window of large language models via positional interpolation, 2023. URL https://arxiv.org/abs/2306.15595.
- Stanley F. Chen and Joshua Goodman. An empirical study of smoothing techniques for language modeling. In *34th Annual Meeting of the Association for Computational Linguistics*, pp. 310–318, Santa Cruz, California, USA, June 1996. Association for Computational Linguistics. doi: 10.3115/981863.981904. URL https://aclanthology.org/P96-1041/.
- Kyunghyun Cho, Bart van Merrienboer, Caglar Gulcehre, Dzmitry Bahdanau, Fethi Bougares, Holger Schwenk, and Yoshua Bengio. Learning phrase representations using rnn encoder-decoder for statistical machine translation, 2014. URL https://arxiv.org/abs/1406.1078.
- Yung-Sung Chuang, Benjamin Cohen-Wang, Shannon Zejiang Shen, Zhaofeng Wu, Hu Xu, Xi Victoria Lin, James Glass, Shang-Wen Li, and Wen tau Yih. Selfcite: Self-supervised alignment for context attribution in large language models, 2025. URL https://arxiv.org/abs/2502.09604.
- Arman Cohan, Franck Dernoncourt, Doo Soon Kim, Trung Bui, Seokhwan Kim, Walter Chang, and Nazli Goharian. A discourse-aware attention model for abstractive summarization of long documents. In *Proceedings of the 2018 Conference of the North American Chapter of the Association for Computational Linguistics: Human Language Technologies, Volume 2 (Short Papers)*, pp. 615–621, New Orleans, Louisiana, June 2018. Association for Computational Linguistics. doi: 10.18653/v1/N18-2097. URL https://aclanthology.org/N18-2097.

```
Anze Xie Ying Sheng Lianmin Zheng Joseph E. Gonzalez Ion Stoica Xuezhe Ma Dacheng Li*, Rulin Shao* and Hao Zhang. How long can open-source llms truly promise on context length?, June 2023. URL https://lmsys.org/blog/2023-06-29-longchat.
```

- Zihang Dai, Zhilin Yang, Yiming Yang, Jaime Carbonell, Quoc V. Le, and Ruslan Salakhutdinov. Transformer-xl: Attentive language models beyond a fixed-length context, 2019. URL https://arxiv.org/abs/1901.02860.
- Kevin Duh, Helena Gomez, and Steven Bethard (eds.). Proceedings of the 2024 Conference of the North American Chapter of the Association for Computational Linguistics: Human Language Technologies (Volume 2: Short Papers), Mexico City, Mexico, June 2024. Association for Computational Linguistics. URL https://aclanthology.org/2024.naacl-short.0/.
- Angela Fan, Mike Lewis, and Yann Dauphin. Hierarchical neural story generation. In *Proceedings* of the 56th Annual Meeting of the Association for Computational Linguistics (Volume 1: Long Papers), pp. 889–898, 2018. URL https://aclanthology.org/P18-1082.
- Lizhe Fang, Yifei Wang, Zhaoyang Liu, Chenheng Zhang, Stefanie Jegelka, Jinyang Gao, Bolin Ding, and Yisen Wang. What is wrong with perplexity for long-context language modeling?, 2025. URL https://arxiv.org/abs/2410.23771.
- Aaron Grattafiori, Abhimanyu Dubey, Abhinav Jauhri, Abhinav Pandey, Abhishek Kadian, Ahmad Al-Dahle, Aiesha Letman, Akhil Mathur, Alan Schelten, Alex Vaughan, Amy Yang, and et al. 2024 Angela Fan. The Ilama 3 herd of models, 2024. URL https://arxiv.org/abs/2407.21783.
- Yuxian Gu, Li Dong, Furu Wei, and Minlie Huang. Minillm: Knowledge distillation of large language models, 2024. URL https://arxiv.org/abs/2306.08543.
- Karl Moritz Hermann, Tom Kocisky, Edward Grefenstette, Lasse Espeholt, Will Kay, Mustafa Suleyman, and Phil Blunsom. Teaching machines to read and comprehend. *NeurIPS*, 2015.
- Sepp Hochreiter and Jürgen Schmidhuber. Long short-term memory. *Neural Computation*, 9(8): 1735–1780, 1997. doi: 10.1162/neco.1997.9.8.1735.
- Ari Holtzman, Jan Buys, Li Du, Maxwell Forbes, and Yejin Choi. The curious case of neural text degeneration. In *International Conference on Learning Representations (ICLR)*, 2020. URL https://arxiv.org/abs/1904.09751.
- Luyang Huang, Shuyang Cao, Lu Wang, and Heng Ji. Efficient attentional models for document summarization. *arXiv preprint arXiv:2104.07241*, 2021.
- Gautier Izacard, Patrick Lewis, Maria Lomeli, Lucas Hosseini, Fabio Petroni, Timo Schick, Jane Dwivedi-Yu, Armand Joulin, Sebastian Riedel, and Edouard Grave. Atlas: Few-shot learning with retrieval augmented language models, 2022. URL https://arxiv.org/abs/2208.03299.
- Haozhe Ji, Pei Ke, Zhipeng Hu, Rongsheng Zhang, and Minlie Huang. Tailoring language generation models under total variation distance, 2023a. URL https://arxiv.org/abs/2302.13344.
- Ziwei Ji, Nayeon Lee, Rita Frieske, Tiezheng Yu, Dan Su, Yan Xu, Etsuko Ishii, Ye Jin Bang, Andrea Madotto, and Pascale Fung. Survey of hallucination in natural language generation. *ACM Computing Surveys*, 55(12):1–38, March 2023b. ISSN 1557-7341. doi: 10.1145/3571730. URL http://dx.doi.org/10.1145/3571730.
- Chen Jia. Adversarial moment-matching distillation of large language models, 2024. URL https://arxiv.org/abs/2406.02959.
- Albert Q. Jiang, Alexandre Sablayrolles, Arthur Mensch, Chris Bamford, Devendra Singh Chaplot, Diego de las Casas, Florian Bressand, Gianna Lengyel, Guillaume Lample, Lucile Saulnier, Lélio Renard Lavaud, Marie-Anne Lachaux, Pierre Stock, Teven Le Scao, Thibaut Lavril, Thomas Wang, Timothée Lacroix, and William El Sayed. Mistral 7b, 2023. URL https://arxiv.org/abs/2310.06825.

- Mandar Joshi, Eunsol Choi, Daniel S. Weld, and Luke Zettlemoyer. Triviaqa: A large scale distantly supervised challenge dataset for reading comprehension, 2017. URL https://arxiv.org/abs/1705.03551.
 - G. Kamradt. Llmtest_needleinahaystack: A needle-in-a-haystack retrieval test for long-context llms. https://github.com/gkamradt/LLMTest_NeedleInAHaystack, 2023.
 - Nora Kassner, Benno Krojer, and Hinrich Schütze. Are pretrained language models symbolic reasoners over knowledge?, 2020. URL https://arxiv.org/abs/2006.10413.
 - Urvashi Khandelwal, He He, Peng Qi, and Dan Jurafsky. Sharp nearby, fuzzy far away: How neural language models use context. In Iryna Gurevych and Yusuke Miyao (eds.), *Proceedings of the 56th Annual Meeting of the Association for Computational Linguistics (Volume 1: Long Papers)*, pp. 284–294, Melbourne, Australia, July 2018. Association for Computational Linguistics. doi: 10.18653/v1/P18-1027. URL https://aclanthology.org/P18-1027/.
 - Tomáš Kočiský, Jonathan Schwarz, Phil Blunsom, Chris Dyer, Karl Moritz Hermann, Gábor Melis, and Edward Grefenstette. The narrativeqa reading comprehension challenge. *TACL*, 2018.
 - Kalpesh Krishna, Erin Bransom, Bailey Kuehl, Mohit Iyyer, Pradeep Dasigi, Arman Cohan, and Kyle Lo. Longeval: Guidelines for human evaluation of faithfulness in long-form summarization, 2023. URL https://arxiv.org/abs/2301.13298.
 - Wojciech Kryściński, Nazneen Rajani, Divyansh Agarwal, Caiming Xiong, and Dragomir Radev. Booksum: A collection of datasets for long-form narrative summarization, 2022. URL https://arxiv.org/abs/2105.08209.
 - Huayang Li, Deng Cai, Jin Xu, and Taro Watanabe. *n*-gram is back: Residual learning of neural text generation with *n*-gram language model, 2022. URL https://arxiv.org/abs/2210.14431.
 - Jiwei Li, Michel Galley, Chris Brockett, Jianfeng Gao, and Bill Dolan. A diversity-promoting objective function for neural conversation models, 2016. URL https://arxiv.org/abs/1510.03055.
 - Xiang Lisa Li, Ari Holtzman, Daniel Fried, Percy Liang, Jason Eisner, Tatsunori B. Hashimoto, Luke Zettlemoyer, and Mike Lewis. Contrastive decoding: Open-ended text generation as optimization. In *Proceedings of the 61st Annual Meeting of the Association for Computational Linguistics* (Volume 1: Long Papers), pp. 12286–12312. Association for Computational Linguistics, 2023.
 - Alisa Liu, Maarten Sap, Ximing Lu, Swabha Swayamdipta, Chandra Bhagavatula, Noah A. Smith, and Yejin Choi. Dexperts: Decoding-time controlled text generation with experts and anti-experts. In *Proceedings of the 59th Annual Meeting of the Association for Computational Linguistics and the 11th International Joint Conference on Natural Language Processing (Volume 1: Long Papers)*, pp. 6691–6706. Association for Computational Linguistics, 2021.
 - Jiacheng Liu, Sewon Min, Luke Zettlemoyer, Yejin Choi, and Hannaneh Hajishirzi. Infini-gram: Scaling unbounded n-gram language models to a trillion tokens, 2025. URL https://arxiv.org/abs/2401.17377.
 - Nelson F. Liu, Kevin Lin, John Hewitt, Ashwin Paranjape, Michele Bevilacqua, Fabio Petroni, and Percy Liang. Lost in the middle: How language models use long contexts, 2023. URL https://arxiv.org/abs/2307.03172.
 - Nikolay Malkin, Zhen Wang, and Nebojsa Jojic. Coherence boosting: When your pretrained language model is not paying enough attention, 2022. URL https://arxiv.org/abs/2110.08294.
 - Stephen Merity, Caiming Xiong, James Bradbury, and Richard Socher. Pointer sentinel mixture models, 2016.
 - Ramesh Nallapati, Bowen Zhou, Cicero dos Santos, Caglar Gulcehre, and Bing Xiang. Abstractive text summarization using sequence-to-sequence rnns and beyond. *arXiv preprint arXiv:1602.06023*, 2016.

```
Shashi Narayan, Shay B. Cohen, and Mirella Lapata. Don't give me the details, just the summary! topic-aware convolutional neural networks for extreme summarization. In Ellen Riloff, David Chiang, Julia Hockenmaier, and Jun'ichi Tsujii (eds.), Proceedings of the 2018 Conference on Empirical Methods in Natural Language Processing, pp. 1797–1807, Brussels, Belgium, October-November 2018. Association for Computational Linguistics. doi: 10.18653/v1/D18-1206. URL https://aclanthology.org/D18-1206/.
```

- Timothy Nguyen. Understanding transformers via n-gram statistics, 2024. URL https://arxiv.org/abs/2407.12034.
- Richard Yuanzhe Pang, Alicia Parrish, Nitish Joshi, Nikita Nangia, Jason Phang, Angelica Chen, Vishakh Padmakumar, Johnny Ma, Jana Thompson, He He, and Samuel R. Bowman. Quality: Question answering with long input texts, yes!, 2022. URL https://arxiv.org/abs/2112.08608.
- Denis Paperno, Germán Kruszewski, Angeliki Lazaridou, Quan Ngoc Pham, Raffaella Bernardi, Sandro Pezzelle, Marco Baroni, Gemma Boleda, and Raquel Fernández. The lambada dataset: Word prediction requiring a broad discourse context, 2016. URL https://arxiv.org/abs/1606.06031.
- Keiran Paster, Marco Dos Santos, Zhangir Azerbayev, and Jimmy Ba. Openwebmath: An open dataset of high-quality mathematical web text, 2023.
- Ofir Press, Noah A. Smith, and Mike Lewis. Train short, test long: Attention with linear biases enables input length extrapolation. *CoRR*, abs/2108.12409, 2021. URL https://arxiv.org/abs/2108.12409.
- Alec Radford, Jeffrey Wu, Rewon Child, David Luan, Dario Amodei, and Ilya Sutskever. Language models are unsupervised multitask learners. https://cdn.openai.com/better-language-models/language_models_are_unsupervised_multitask_learners.pdf, 2019.
- Yasaman Razeghi, Robert L Logan IV, Matt Gardner, and Sameer Singh. Impact of pretraining term frequencies on few-shot numerical reasoning. In Yoav Goldberg, Zornitsa Kozareva, and Yue Zhang (eds.), *Findings of the Association for Computational Linguistics: EMNLP 2022*, pp. 840–854, Abu Dhabi, United Arab Emirates, December 2022. Association for Computational Linguistics. doi: 10.18653/v1/2022.findings-emnlp.59. URL https://aclanthology.org/2022.findings-emnlp.59/.
- Holger Schwenk, Vishrav Chaudhary, Shuo Sun, Hongyu Gong, and Francisco Guzmán. Wikimatrix: Mining 135m parallel sentences in 1620 language pairs from wikipedia, 2019. URL https://arxiv.org/abs/1907.05791.
- Pratyusha Sharma, Jordan T Ash, and Dipendra Misra. The truth is in there: Improving reasoning in language models with layer-selective rank reduction. *arXiv preprint arXiv:2312.13558*, 2023.
- Jianlin Su, Yu Lu, Shengfeng Pan, Bo Wen, and Yunfeng Liu. Roformer: Enhanced transformer with rotary position embedding. *CoRR*, abs/2104.09864, 2021. URL https://arxiv.org/abs/2104.09864.
- Simeng Sun, Kalpesh Krishna, Andrew Mattarella-Micke, and Mohit Iyyer. Do long-range language models actually use long-range context? In *Findings of the Association for Computational Linguistics: ACL-IJCNLP 2021*, pp. 3306–3317. Association for Computational Linguistics, 2021.
- Gemma Team, Thomas Mesnard, Cassidy Hardin, Robert Dadashi, Surya Bhupatiraju, Shreya Pathak, Laurent Sifre, Morgane Rivière, Mihir Sanjay Kale, Juliette Love, Pouya Tafti, Léonard Hussenot, Pier Giuseppe Sessa, Aakanksha Chowdhery, Adam Roberts, Aditya Barua, and et al. Alex Botev. Gemma: Open models based on gemini research and technology, 2024. URL https://arxiv.org/abs/2403.08295.
- Bram van der Poel, Zheng Li, Shashi Narayan, Ramesh Nallapati, Kathleen McKeown, and Trung Bui. Mutual information decoding for abstractive summarization. In *Proceedings of the 2022 Conference on Empirical Methods in Natural Language Processing*, pp. 5850–5866. Association for Computational Linguistics, 2022.

- Ashish Vaswani, Noam Shazeer, Niki Parmar, Jakob Uszkoreit, Llion Jones, Aidan N Gomez, Łukasz Kaiser, and Illia Polosukhin. Attention is all you need. In *Advances in neural information processing systems*, pp. 5998–6008, 2017.
- Weizhi Wang, Li Dong, Hao Cheng, Xiaodong Liu, Xifeng Yan, Jianfeng Gao, and Furu Wei. Augmenting language models with long-term memory, 2023. URL https://arxiv.org/abs/2306.07174.
- An Yang, Baosong Yang, Binyuan Hui, Bo Zheng, Bowen Yu, Chang Zhou, Chengpeng Li, Chengyuan Li, Dayiheng Liu, Fei Huang, Guanting Dong, Haoran Wei, Huan Lin, and et al. Jialong Tang. Qwen2 technical report, 2024. URL https://arxiv.org/abs/2407.10671.
- Zhilin Yang, Peng Qi, Saizheng Zhang, Yoshua Bengio, William W. Cohen, Ruslan Salakhutdinov, and Christopher D. Manning. Hotpotqa: A dataset for diverse, explainable multi-hop question answering, 2018. URL https://arxiv.org/abs/1809.09600.
- WJ Youden. Index for rating diagnostic tests. Cancer, 3(1):32–35, 1950.
- Zhenyu Zhang, Runjin Chen, Shiwei Liu, Zhewei Yao, Olatunji Ruwase, Beidi Chen, Xiaoxia Wu, and Zhangyang Wang. Found in the middle: How language models use long contexts better via plug-and-play positional encoding, 2024. URL https://arxiv.org/abs/2403.04797.
- Zheng Zhao, Emilio Monti, Jens Lehmann, and Haytham Assem. Enhancing contextual understanding in large language models through contrastive decoding. *arXiv preprint arXiv:2405.02750*, 2024.
- Ming Zhong, Da Yin, Tao Yu, Ahmad Zaidi, Mutethia Mutuma, Rahul Jha, Ahmed Hassan Awadallah, Asli Celikyilmaz, Yang Liu, Xipeng Qiu, and Dragomir Radev. Qmsum: A new benchmark for query-based multi-domain meeting summarization, 2021. URL https://arxiv.org/abs/2104.05938.
- Yuxuan Zhou, Margret Keuper, and Mario Fritz. Balancing diversity and risk in llm sampling: How to select your method and parameter for open-ended text generation, 2025. URL https://arxiv.org/abs/2408.13586.
- Wenhong Zhu, Hongkun Hao, Zhiwei He, Yiming Ai, and Rui Wang. Improving open-ended text generation via adaptive decoding, 2024. URL https://arxiv.org/abs/2402.18223.

A SUMMARY OF PAPER'S NOTATIONS

756

758

775 776 777

778 779

781

782

783

784

785

786

787

788

789

790

791

792

793

794 795

796

797

798

799

800

801

802

803

804

805

806

807

808

809

Table 2 provides a summary of the notation used in this paper.

Symbol	Description
	Scalar / vector (boldface)
[i]	<i>i</i> -th entry of vector
[i]:j	Index set $\{i, i+1, \ldots, j\}$
[-l]	Suffix of of length l
\mathcal{V}	Vocabulary of tokens, $V = \mathcal{V} $
$\mathbf{s} = [t_1, \dots, t_n]$	Tokenized document of length n
$egin{array}{c} \mathbf{s}_{[i]} \ \Delta^n \end{array}$	Prefix of s of length i
$\mathring{\Delta}^{\check{n}}$	Probability simplex in \mathbb{R}^n
$Top_k(\cdot)$	Indices of k largest entries of a vector;
$\pi_{ heta}(\mathbf{s})$	LM distribution over V given context s
$\Delta Conf(\mathbf{s})$	Confidence = gap between top-1 and top-2 probabilities
LSDS(s)	Long-short distribution shift (JSD of short vs full context)
LSPS(t s)	Long-short probability shift for token t in sequence s

Table 2: Notation used throughout the paper.

B DISCUSSION AND RELATED WORK

Pursuit of Long Context: Capturing dependencies that extend beyond a few tokens has been a long-standing difficulty in language modeling. Early statistical and neural models either truncated context to short n-grams or attempted to maintain memory through recurrence, but both approaches faced limitations with sparsity or vanishing gradients (Chen & Goodman, 1996; Bengio et al., 2003; Hochreiter & Schmidhuber, 1997; Cho et al., 2014). The Transformer architecture (Vaswani et al., 2017) marked a turning point, with self-attention providing a scalable mechanism for integrating information from across the entire input. Contemporary open-access models such as LLaMA 3 (Grattafiori et al., 2024), Mistral (Jiang et al., 2023), Owen2 (Yang et al., 2024), and Gemma (Team et al., 2024) support context lengths from 8K to 128K tokens, large enough to encode entire novels in a single pass. To make such extensions feasible, architectural innovations like rotary position encodings (RoPE) (Su et al., 2021), attention linear biases (ALiBi) (Press et al., 2021), and position interpolation (Chen et al., 2023) enable models to extrapolate beyond their training horizon, while retrieval-augmented designs (Borgeaud et al., 2022; Izacard et al., 2022; Wang et al., 2023) surface or cache relevant information as an alternative to enlarging the raw attention window. Yet, greater architectural capacity does not imply that models make effective use of long-range context at inference time—the focus of our analysis.

Context Utilization: Despite larger context windows, studies show that LMs often do not utilize long-range information. Khandelwal et al. (2018) characterize predictions as "sharp nearby, fuzzy far away," with sensitivity concentrated in the most recent span, while Sun et al. (2021) demonstrate that only a small fraction of tokens benefit from context beyond the first few thousand tokens. Such works emphasize the inherent recency bias in language models. Complementing these results, Liu et al. (2023) document a strong positional bias—models attend to evidence at the edges of long prompts while neglecting the middle, a challenge further analyzed by Zhang et al. (2024), who trace the effect to rotary positional encodings and propose positional modifications to resolve it. To mitigate these limitations, document retrieval approaches have been proposed to surface relevant passages at inference time (Borgeaud et al., 2022; Izacard et al., 2022), while recent work emphasizes the role of training data quality in enabling long-context utilization. In particular, Chen et al. (2025) introduce an attention-based dependency measurement framework (LADM) to identify long documents with strong internal dependencies, showing that selecting such high-quality data for continual pretraining substantially improves long-context performance. Beyond interventions at the system and data level, attribution-based methods such as Chuang et al. (2025) directly test the necessity and sufficiency of context spans, offering a finer-grained perspective on how LLMs actually use long inputs. Similarly, we study the utilization of context from a minimal required sub-context viewpoint, showing that

majority of next token queries utilize very local information. Additionally, we provide methodology to identify the minimal required sub context and while distinguishing between long-short context queries.

Contrastive Decoding: Beyond architectural and data-level interventions, several ad hoc inferencetime methods aim to improve token generation. Early work encouraged generation that depends more strongly on the given context rather than defaulting to frequent or generic outputs. (Li et al., 2016) propose a mutual-information—based objective for dialogue generation to discourage generic responses, while (Brown et al., 2020) address this issue in multiple-choice QA by normalizing candidate likelihoods against unconditional probabilities, thereby encouraging context-dependent answers. Malkin et al. (2022) introduced coherence boosting, a general inference-time method that reweights the next-token distribution to favor predictions supported by the full long context by explicitly contrasting it against the distribution induced by a shortened context. van der Poel et al. (2022) proposed an entropy-aware decoding strategy for summarization, where the scoring function switches to pointwise mutual information between the source document and the next token when model uncertainty is high, thereby discouraging hallucinations and reducing the tendency to select high-frequency but unsupported tokens. Similar to Malkin et al. (2022) but operating on a logit level, Duh et al. (2024) introduce Context-Aware Decoding (CAD), an inference-time method designed to reduce hallucinations by explicitly amplifying the difference between a model's output probabilities with and without the provided context. Much of this line of research grows out of the broader family of contrastive decoding methods (Li et al., 2023; Zhao et al., 2024; Liu et al., 2021) which are designed for ad hoc modification toe next token distribution to improve language generation. For our case, instead of focusing on performance we first provide an objective study of short context bias of language and use our findings to design intuitive and explainable algorithms to to identify long long contexts, relevant tokens and how to combine this knowledge to help improve generation.

n-gram and its short context relevance: Recent work has revisited n-gram models as complements or interpretive tools for neural language models. Li et al. (2022) showed that residual learning with a small n-gram LM can regularize neural text generation and reduce hallucination. More recently, Liu et al. (2025) introduced Infini-gram, which scales n-gram models to trillions of tokens and supports unbounded context length using suffix arrays, enabling both strong next-token prediction and new diagnostic analyses of neural LMs. In parallel, Nguyen (2024) argue for understanding Transformers through the lens of n-grams, showing that simple n-gram rulesets can approximate a majority of model predictions (e.g., covering 68–79% of top-1 predictions across benchmarks). Given that n-grams are inherently short-range models—even Infini-gram typically captures at most 32-token dependencies—the fact that they achieve performance comparable to Transformers on standard text suggests a structural bias in language toward short-context sufficiency, which allows such models to achieve moderate success despite their limited horizon. Our observations regarding the overwhelming prevalence of inherently short contexts in natural language can help explain the reason behind the success of such methods which rely on local information using n-grams for generation.

Long Context Evaluation: Much of the evaluation of a model's contextual understanding has focused on tasks such as question answering, retrieval, and needle-in-the-haystack probing, evaluated on datasets such as NarrativeQA (Kočiský et al., 2018), TriviaQA (Joshi et al., 2017), QuALITY (Pang et al., 2022), and LongBench (Bai et al., 2024). While these benchmarks test a model's ability to extract specific information from distant context, they differ from standard language modeling and tend to be highly task-specific. A recent study by Fang et al. (2025) proposes a method for identifying tokens with long-context dependencies and encourages training-time metrics that distinguish such tokens. While their work focuses on a binary classification of long- vs. short-context tokens, we adopt a more fine-grained perspective: treating the language model as a probabilistic oracle and estimating the minimal context required for each next-token prediction in natural text. Additionally, we provide methods for detection of long-context and tokens with long-context relevance without requiring the actual ground truth next token, making our methods applicable during inference.

Decoding Strategies: Given our assumption that language models serve as strong proxies for language understanding, it is important to account for the decoding strategy used during inference. A growing body of research has shown that different sampling methods—such as greedy decoding, top-k sampling (Radford et al., 2019; Fan et al., 2018), nucleus (p) sampling (Holtzman et al., 2020), and adaptive techniques (Basu et al., 2021; Zhu et al., 2024)—can substantially influence output diversity, factuality, and calibration. Greedy decoding in particular has been shown to produce degenerate or overly deterministic outputs, while adaptive and dynamic approaches aim to adjust

sampling entropy and generate a high-quality, contextually valid subset of tokens (Holtzman et al., 2020; Zhu et al., 2024; Basu et al., 2021). When treating the language model as a statistical oracle for analyzing context usage, it is essential to consider how decoding strategy influences conclusions about effective context length. This perspective may help improve the practical utility of methods such as Fang et al. (2025), which focus primarily on a single sample from the next-token distribution to classify tokens by their context length requirements. Accordingly, we provide a dedicated analysis of how decoding strategies impact context dependence in next-token prediction and its relation to short-long context detection.

C ADDITIONAL RESULTS ON MCL

C.1 Ablation Results: Model Size and onfidence threshold δ

We perform ablation experiments on MCL results regarding model size and the impact of confidence threshold δ in Fig. 9 and Fig. 10 respectively. Observations further confirm that the short-context dominance hypothesis appears irrespective of experimental setup.

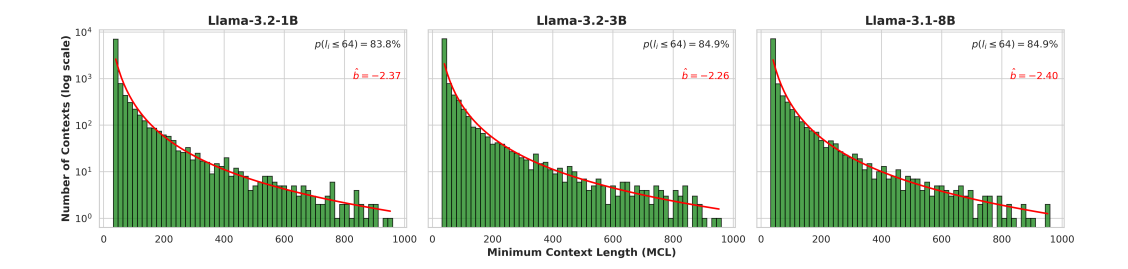


Figure 9: **Impact of model size:** Similar setup to Fig. 2 but Llama models with different sizes. We can see that the distribution of MCL behavior doesn't change across different models sizes of 1,3 and 7 billion parameter sizes.

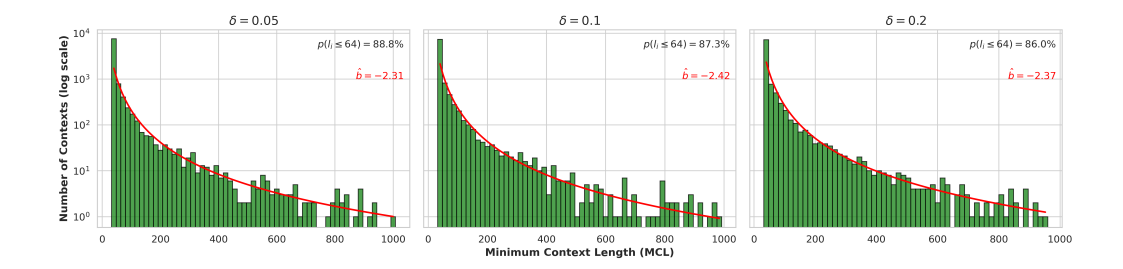


Figure 10: **Impact of confidence threshold** δ : Similar setup to Fig. 2 with Llama-3 8B running MCL experiments with different values of $\delta \in \{0.05, 0.1, 0.2\}$. Results suggest that the observation is confidence threshold of the MCL value.

C.2 LANGUAGE AND DOMAIN RESULTS

We conduct two sets of generalization experiments to confirm the robustness of the short-context dominance. First, we examine the language effect by running inference on Wikipedia article translations in Arabic, Chinese, French, German, Korean, Russian, and Thai, using the Qwen2-7B model (Yang et al., 2024). These texts are sampled from the Wikimedia dataset (Schwenk et al., 2019), and follow the same selection and truncation procedure as our English WikiText documents. Results in Table 3 and Fig. 11 confirm that the reliance on short context is preserved across languages, with similarly highly skewed token count distributions and consistent exponential fits.

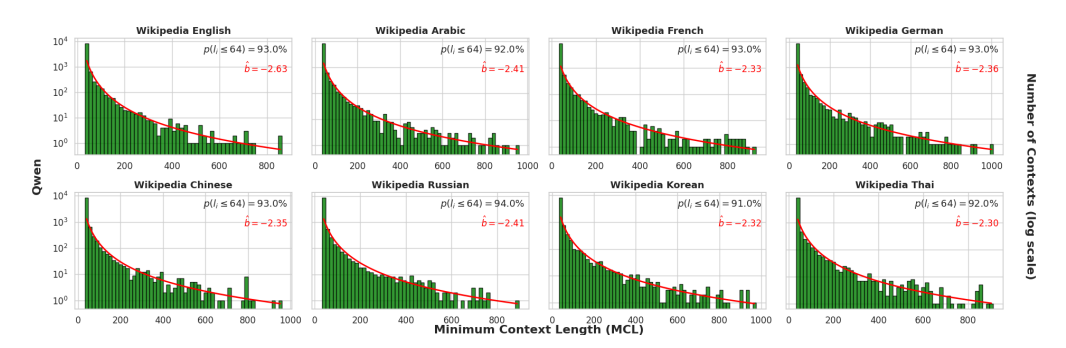


Figure 11: **Distribution of MCL on Different Languages:** Similar setup to Fig. 2 but performed over a set of articles from Wikipedia and their respective translations into different languages. We see that the same trend appears irrespective of target language. This analysis was conducted on Qwen-2 model only.

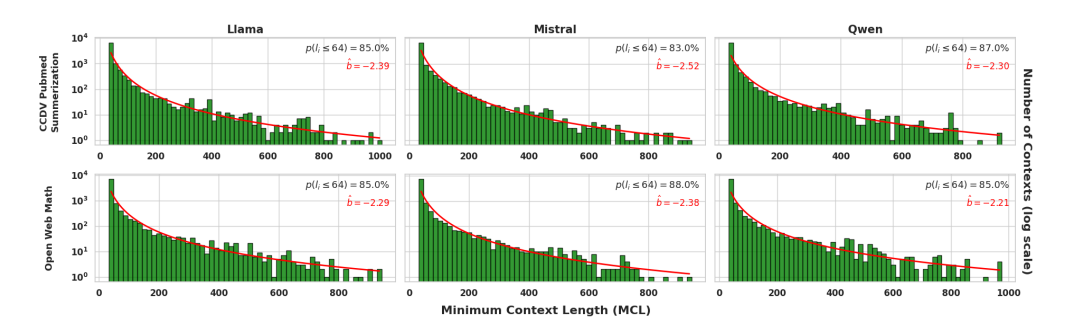


Figure 12: **Distribution of MCL on Math And Medical Datasets:** This figure shows the distribution of MCL values over two specialized domains: medical (CCDV PubMed Summarization) and mathematical (Open Web Math), with a similar setup as Fig. 2. The MCL distribution consistently follows the same trend across both domains and all three models. This suggests that the observed phenomenon is robust to changes in domain knowledge.

Second, to evaluate domain knowledge effects, we test on two specialized datasets: CCDV PubMed Summarization (Cohan et al., 2018) for biomedical abstracts, and Open Web Math (Paster et al., 2023) for mathematical content, across all 3 models: LLaMA-3-8B (Grattafiori et al., 2024), Mistral-7B-Instruct (v0.1) (Jiang et al., 2023) and Qwen2-7B (Yang et al., 2024). As shown in Fig. 12, the short-context dominance pattern remains intact across both domains and models. This suggests models' reliance on local context persist even when dealing with knowledge-intensive content.

D DAMCL

D.1 MOTIVATIONS ON DAMCL

Table 3: Estimated power-law exponents (\hat{b}) for MCL distributions on the Wikimedia dataset using Qwen.

Language	\hat{b}
English	-2.63
Arabic	-2.41
French	-2.33
German	-2.36
Chinese	-2.35
Russian	-2.41
Korean	-2.32
Thai	-2.30

In Sec. 3, we posed the question of determining the minimum subcontext prefix needed to predict the next token in a given dataset. A key limitation of this formulation is that it is constrained by the specific realization of the natural language distribution underlying that dataset.

Put simply, given a context, there are often multiple valid next tokens—valid in terms of the underlying (but unknown) distribution of natural language. While we cannot access this true distribution, we have treated pretrained LLMs as statistical oracles. However, in defining MCL in Definition 1, we constrain these oracles by evaluating them against only the actual next to-

ken from the dataset. Furthermore, we rely solely on greedy decoding, which outputs a single token, thereby underutilizing the model's full predictive distribution as a language oracle. We summarize the issues as follows:

- 1. Even if the oracle's top-1 prediction does not match the next token in the source text, i.e., $\mathsf{Top}_1(\mathbf{s}_{[-l:]}) \neq t$, this does not invalidate the model's output or imply a lack of contextual understanding. As shown in Fig. 13, the model assigns high probability to several plausible continuations, even if the dataset token is not ranked first. This suggests that relying solely on the dataset token may mislead any contextlength detection method.
- 2. Using the Top-1 token from the sampling distribution is not always a reliable way to evaluate next-token prediction, as greedy decoding often results in low-quality or repetitive out

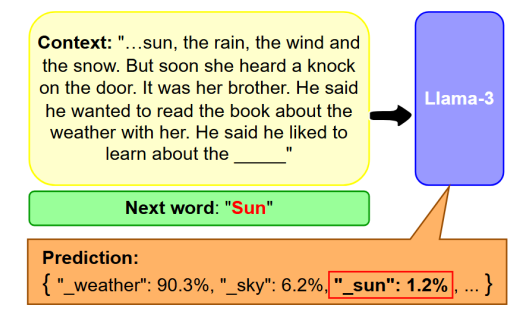


Figure 13: An example illustrating the limitations of relying on greedy sampling and the actual next token: the Top-1 prediction is a valid response but does not match the ground-truth token. Metrics like MCL may overlook such cases, misidentifying the minimal required context.

puts (Holtzman et al., 2020). More recent sampling strategies instead aim to identify a set of valid next tokens (Zhu et al., 2024; Zhou et al., 2025), shifting the focus away from single-token probabilities toward broader support coverage.

These issues motivate the need for a broader definition of MCL—one that 1) relies on the model's own next-token distribution rather than the actual next token, and 2) accounts for the sampling strategy used during inference. The goal of DaMCL is to mitigate these limitations and offer a more faithful metric for contextual understanding.

D.2 ADDITIONAL METRICS FOR DAMCL

In addition the main JSD metric used in Sec. 4, we perform the same experiments with a number of other common metrics used to represent similarity between sets and distributions. For the given distributions $P,Q\in\Delta^{\mathcal{V}}$ in the $|\mathcal{V}|$ -dimensional simlex we use the following standard distributional similarity metrics:

$$\label{eq:TVD} \mbox{Total Variation Distance:} \quad \mbox{TVD}(P,Q) := \frac{1}{2} \|P - Q\|_1 \,,$$

$$\mbox{Kullback-Leibler Divergence:} \quad \mbox{KL}(P\|Q) := \sum_{v \in \mathcal{V}} P(v) \log \frac{P(v)}{Q(v)} \,.$$

These metrics are widely employed in applications such as knowledge distillation and in assessing performance degradation of large language models under various conditions (Gu et al., 2024; Ji et al., 2023a; Jia, 2024). Exploring alternative, less conventional metrics remains an avenue for future work.

Furthermore, we consider metrics which rely on the inclusions of tokens in the support set rather than the probability distributions. To this end, we define define the Recall, Precision and F1 metric from set P to set Q as:

$$\begin{split} \operatorname{Recall}\left(P\mid Q\right) := \frac{|P\cap Q|}{|Q|} \in [0,1] \qquad \operatorname{Prec}\left(P\mid Q\right) := \frac{|P\cap Q|}{|P|} \in [0,1]\,, \\ \operatorname{F1}\left(P\mid Q\right) := \frac{2\times \operatorname{Recall}\left(P\mid Q\right) \times \operatorname{Prec}\left(P\mid Q\right)}{\operatorname{Recall}\left(P\mid Q\right) + \operatorname{Prec}\left(P\mid Q\right)} \in [0,1]\,. \end{split}$$

Recall measures the proportion of elements in set Q that are also present in set P, i.e., how much of Q is recovered by P. **Precision**, on the other hand, quantifies the proportion of elements in P that are relevant—those that also belong to Q. A Recall of 1 implies $Q \subseteq A$, meaning all elements

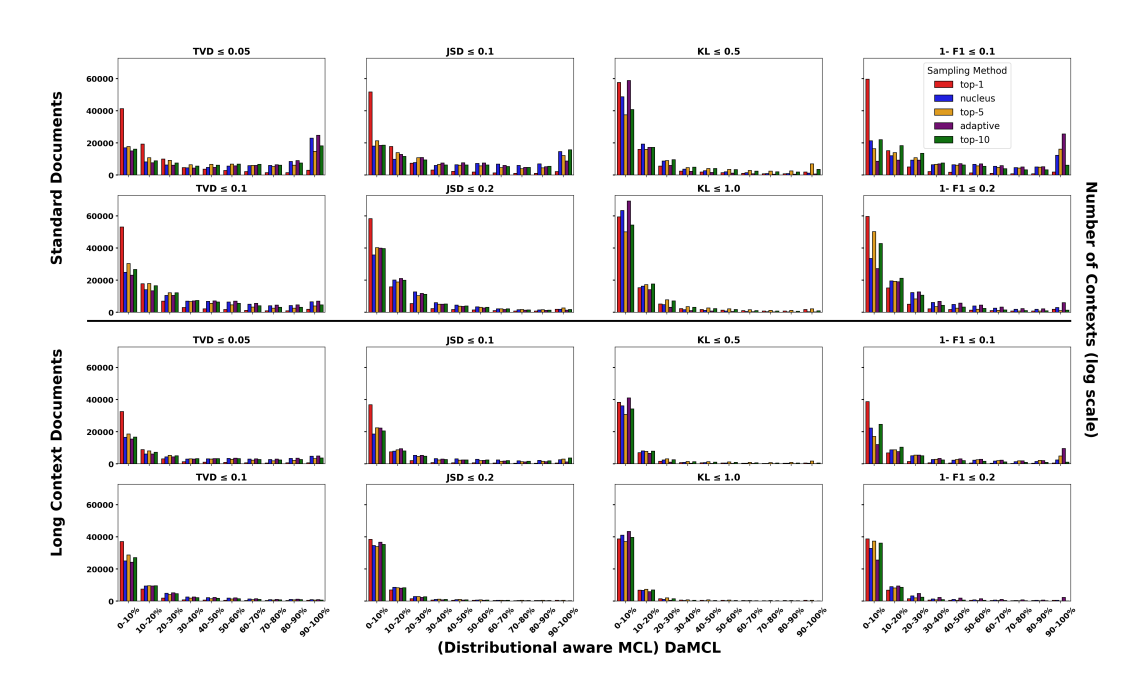


Figure 14: **Distribution of DaMCL:** The distributionally-aware MCL is defined using a range of metrics applied with relative thresholds. Results are presented separately for standard documents (top row) and long-context documents (bottom row) to highlight potential differences in behavior. While the overall trend resembles the exponentially decaying pattern observed in standard MCL (see Fig. 2), the choice of metric and threshold clearly influences the outcome. Each subplot reflects results aggregated over all model—dataset combinations, as only minor deviations were observed across different configurations under identical hyperparameters.

of Q are captured by P. Conversely, a Precision of 1 implies $P \subseteq Q$, indicating that P contains no extraneous elements outside of Q. The $\mathbf{F1}$ score is defined as the harmonic mean of Recall and Precision, providing a balanced measure that accounts for both. These definitions are standard in the information-theoretic analysis of set similarity and coverage. For this set, we focus on the F1 score, specifically calculating 1-F1 in order to match the preference for smaller values, similar to the JSD, TVD and KL metrics.

In comparison to JSD, we observe that both TVD and KL exhibit similar bimodal distribution trends under stricter threshold values. Moreover, neither metric shows substantially different behavior across sampling strategies. In contrast, the $1-\mathsf{F}1$ metric, while following the same general trend, displays several notable deviations. Specifically, the distributions tend to be more heavily biased toward requiring longer subcontexts to meet threshold requirements. This effect is particularly pronounced in smaller documents when using adaptive sampling, where DaMCL values skew more strongly toward full-context reliance under stricter thresholds.

Our focus on JSD is motivated by several desirable properties that make it especially well-suited for DaMCL. Notably, JSD is a proper distance metric and satisfies the triangle inequality. Furthermore, as a smoothed and symmetric variant of KL divergence, JSD is generally more robust to noise and less sensitive to zero-probability

Table 4: MCL vs. DaMCL results for LLaMA-3. GovReport is shown at 96 tokens, CNN and Wiki at 64 tokens.

Dataset	MCL (%)	DaMCL (%)
GovReport (≤ 96)	75.19	36.36
News Articles (≤ 64)	80.52	45.43
Wikipedia (≤ 64)	78.15	31.65

events—properties that are particularly beneficial when working with LLM next-token distributions. Nonetheless, we acknowledge that further exploration of alternative metrics may reveal additional insights or complementary advantages. We leave this to future work.

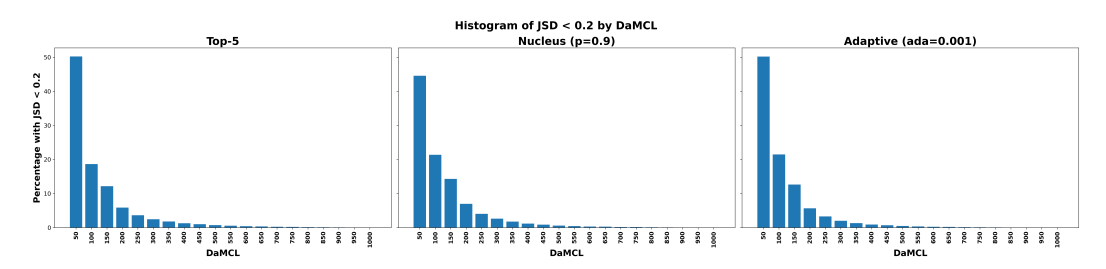


Figure 15: **DaMCL with fixed sub-contexts**: Similar to Fig. 4, but under difference decoding methods.

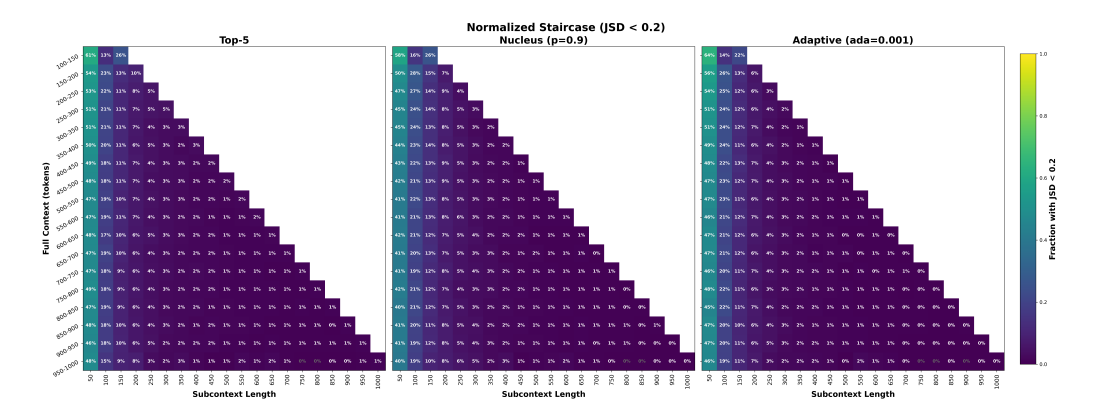


Figure 16: **DaMCL heatmap with fixed sub-contexts**: Each row represents contexts of a certain size and each column represents sub-contexts which were tested for $JSD \le 0.2$.

D.3 DAMCL WITH FIXED SUB-CONTEXT

In order to further analyze the behavioral change of DaMCL compared to MCL, where a larger number of contexts rely on the full length, we perform a number of experiments and analysis using fixed subcontext lengths. First note the results provided in Table 4 which indicate that compared to MCL, a smaller portion of context queries can be resolved with the short sub-contexts.

Looking at Fig. 4 and its more complete counterpart Fig. 15 we still see the bias towards shorter context but less than that of MCL. Once again for ease of computation, we change the sub-context increments to 50 tokens instead of 32. Instead of looking at all contexts sizes at the same time, we can analyze each context size group separately.

In Fig. 3, we can see that for longer context, very rarely does the the model require the full context to have a close distribution in terms of JSD. Notably, for shorter contexts $|\mathbf{s}| \leq 200$, its much more likely for the model to require the full context and this could be a reason behind our observation of the bimodal DaMCL values on Fig. 14.

E LONG-CONTEXT SEQUENCE DETECTION

E.1 ADDITIONAL SETUPS AND ORACLES

Here, we provide further experiments with various setups and oracles that complement the results in Section 5. These additional studies reinforce the effectiveness of Jensen–Shannon Distance (JSD) as a robust detector of long-context dependence.

E.1.1 CONTROLLED VALIDATION EXPERIMENT ON LONGEVAL TASK

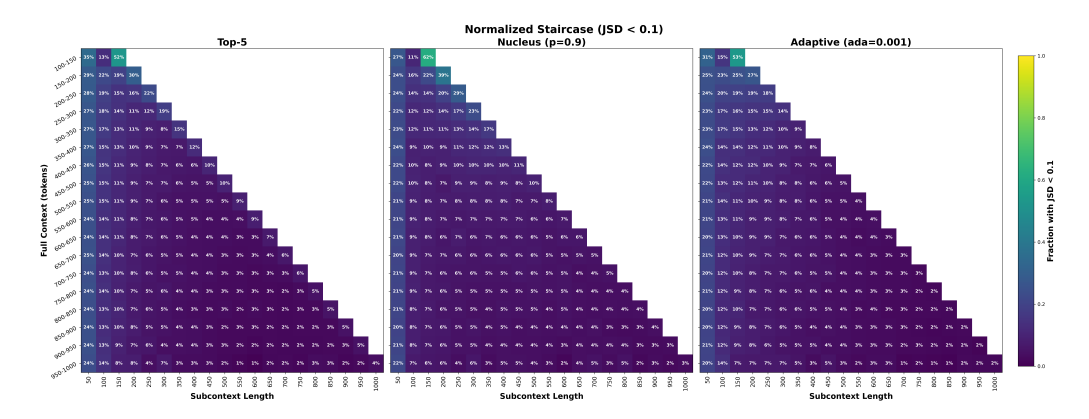


Figure 17: **DaMCL** heatmap with fixed sub-contexts: $JSD \le 0.1$.

Using the LongEval benchmark (Dacheng Li* & Zhang, 2023), we construct prompts containing multiple register lines, each with a *line_id* and *<REGISTER_CONTENT>* value, where the model must identify specific content. We create two types of queries with known ground-truth labels: *short-context* queries where the answer (a *line_id*) appears in the last 32 tokens, and *long-context* queries where the answer (a *<REGISTER_CONTENT>*) requires information from the full context. We conduct the experiments on three models: LLaMA-3-8B (Grattafiori et al., 2024), Mistral-7B-Instruct (v0.2) (Jiang et al., 2023), and Qwen2-7B (Yang et al., 2024). As shown in Figure 20, across all models, we observe the same distributional trend, confirming the robustness of the results.

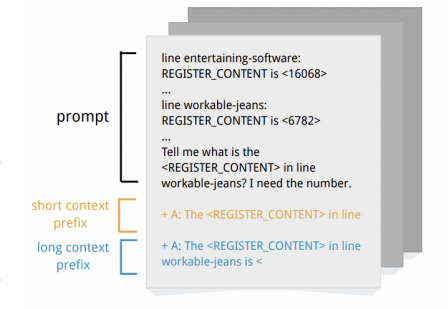


Figure 18: An example of the controlled validation experiment setup on the LongEval benchmark.

E.1.2 NEEDLE-IN-A-HAYSTACK EXPERIMENT ON GENERAL TEXT

We next adapt a needle-in-a-haystack (NIAH) style setup to general text. Following the classic needle-in-a-haystack test by Kamradt (2023), given a natural context, we insert a needle statement with a randomly generated 6-digit number: "The magic number is xxxxxxx" at a specific position in the text. At the end of the document, we append a query prompt: "The magic number mentioned in the provided text is", expecting the model to output the correct number from the needle. If the needle statement is placed within the final 32 tokens, the answer is recoverable from the local suffix, and we label the case as a short context. Otherwise, when the needle is inserted far away, answering requires long-range recall, and we label it as a long context. We only retain cases where the model outputs the correct number, ensuring the prediction truly relies on the inserted statement rather than hallucination.

Figure 19 presents the JSD distributions under this setup, showing that long-context tokens yield consistently higher JSD values compared to short-context tokens, validating JSD as a detector in this natural-text scenario.

E.1.3 PRIOR-WORK ORACLE (LSD/LCL) ON GENERAL TEXT

As described in Section 5, we evaluate a *prior-work oracle* detector that follows the log-probability intervention from Fang et al. (2025). The oracle Long-Short Difference (LSD) and Long-Context Likelihood (LCL) are defined as follows:

For sequence s with corpus next-token t, and a language model P_{θ} ,

$$LSD_{\theta}(\mathbf{s}|t) = \log P_{\theta}(t \mid \mathbf{s}) - \log P_{\theta}(t \mid \mathbf{s}_{[-32:]})$$
 (2)

and

$$LCL_{\theta}(\mathbf{s}|t) = \log P_{\theta}(t \mid \mathbf{s}) \tag{3}$$

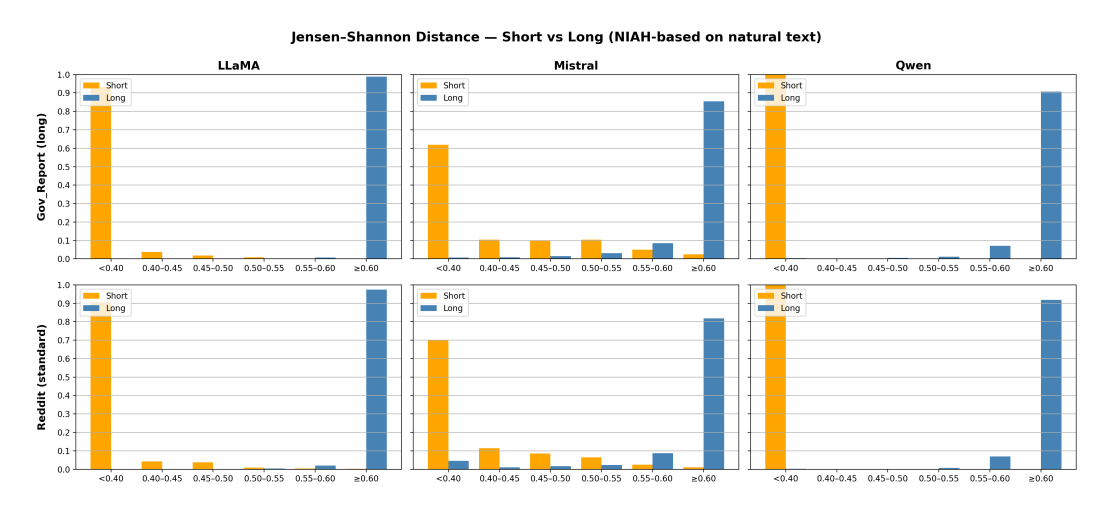


Figure 19: **NIAH-based experiment on General text result:** LSDS distribution across three models (LLaMA, Mistral, Qwen) on long-context dataset (GovReport) and standard-length context (Reddit), each with 10000 samples. Each subplot shows the proportion of tokens falling into fixed JSD bins.

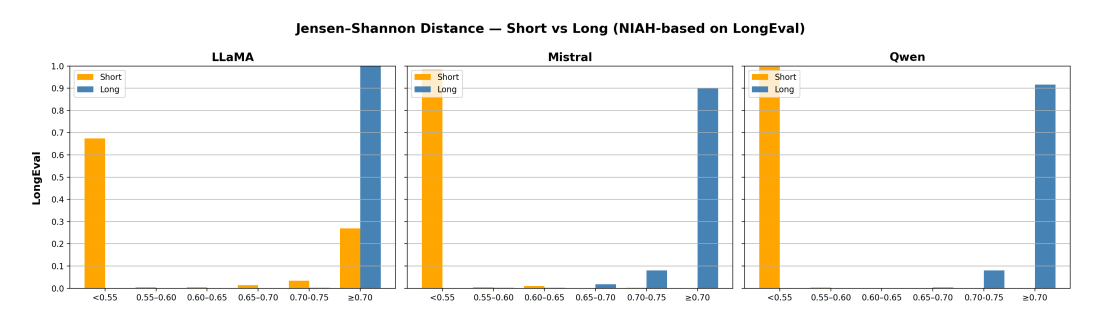


Figure 20: Controlled validation experiment on LongEval task result: LSDS distribution across three models (LLaMA, Mistral, Qwen) on the LongEval synthetic benchmark. Each subplot shows the proportion of tokens falling into fixed JSD bins.

Figure 21 shows the per-model distributions of LSDS for LLaMA-3-8B, Mistral-7B-Instruct, and Qwen2-7B on the same data used in the main body. The per-model trends mirror the pooled result: using a threshold of $\tau=0.6$, we find consistently that 80-90% of oracle-labeled long-context sequences achieve LSDS (s) ≥ 0.6 , while fewer than 5-10% of short-context sequences exceed this threshold.

E.1.4 MCL ORACLE ON GENERAL TEXT

Additionally, we evaluate our MCL Oracle on general text. Following the definition and computation procedure in Section 3, we compute the MCL of each given context. Tokens with small MCL values (≤ 32) are classified as short-context, while those requiring larger suffixes (> 32) are classified as long-context. A limitation of this approach is that the MCL framework does not always yield a finite value, leaving some contexts unlabeled.

We then compare the JSD distributions of tokens across the two categories. Figure 22 shows that the detected trend is still preserved.

E.2 ABLATION ON NUCLEUS SAMPLING PARAMETER (p)

In this section, we examine how varying the nucleus sampling parameter p influence our LSDS and the resulting JSD threshold. We report results for 4 settings: no nucleus sampling, p = 0.95, p = 0.90, and p = 0.80. We conduct the experiment with Mistral-7B-Instruct (v0.2) (Jiang et al.,

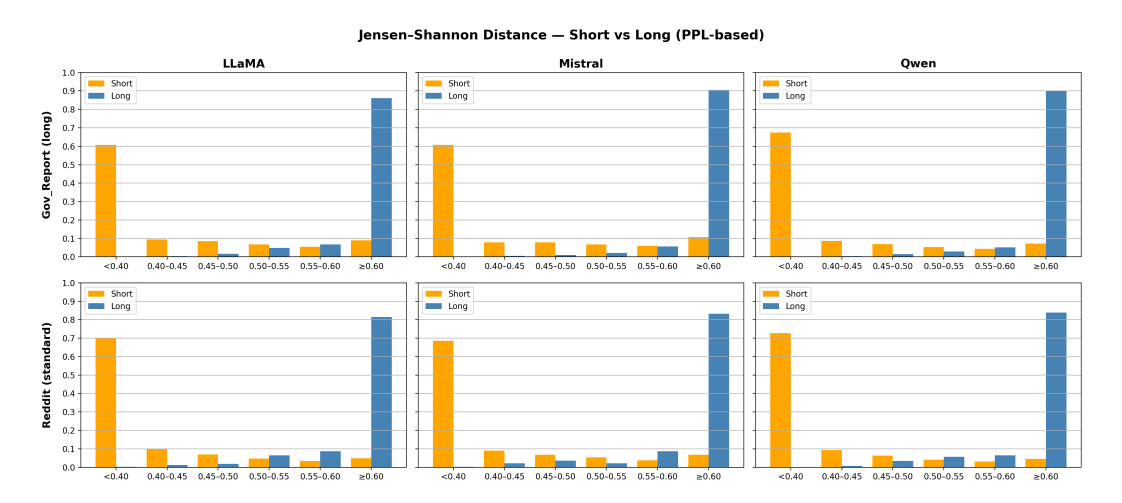


Figure 21: **Prior-work oracle (LSD/LCL) on general text result:** LSDS distribution across three models (LLaMA, Mistral, Qwen) on long-context dataset (GovReport) and standard-length context (Reddit), each with 10000 samples. Each subplot shows the proportion of tokens falling into fixed JSD bins.

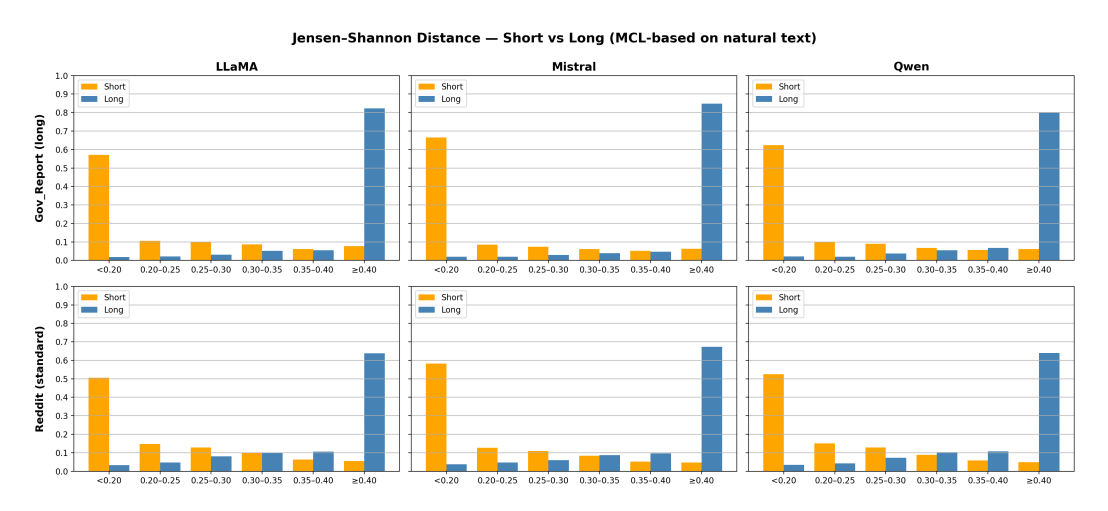


Figure 22: **MCL oracle on general text result:** LSDS distribution across three models (LLaMA, Mistral, Qwen) on long-context dataset (GovReport) and standard-length context (Reddit), each with 10000 samples. Each subplot shows the proportion of tokens falling into fixed JSD bins.

2023) on 5000 contexts randomly selected from Government Report (Huang et al., 2021), with full context length ranging from 100–1000 tokens. The ground truth oracle we use here is *Prior Work Oracle* as introduced in Sec. 5.

Across all settings, we observe that the separation between short- and long-context distribution is preserved (see Figure 23). Regardless of p, short-context examples consistently concentrate in low JSD bins (< 0.40), while long-context examples dominate the high JSD bins (≥ 0.60). However, the optimal detection thresholds vary slightly depending on p value.

To quantitatively assess performance, we compute the maximized Youden's J statistic (Youden, 1950):

$$J = \max_{\theta} \left\{ \mathsf{TPR}(\theta) - \mathsf{FPR}(\theta) \right\}$$

where TPR is the true positive rate and FPR is the false positive rate, and θ is the decision threshold. Unlike accuracy, which can be biased by imbalanced class distributions, J simultaneously accounts for both sensitivity (true positive rate) and specificity (true negative rate). In our case, detecting

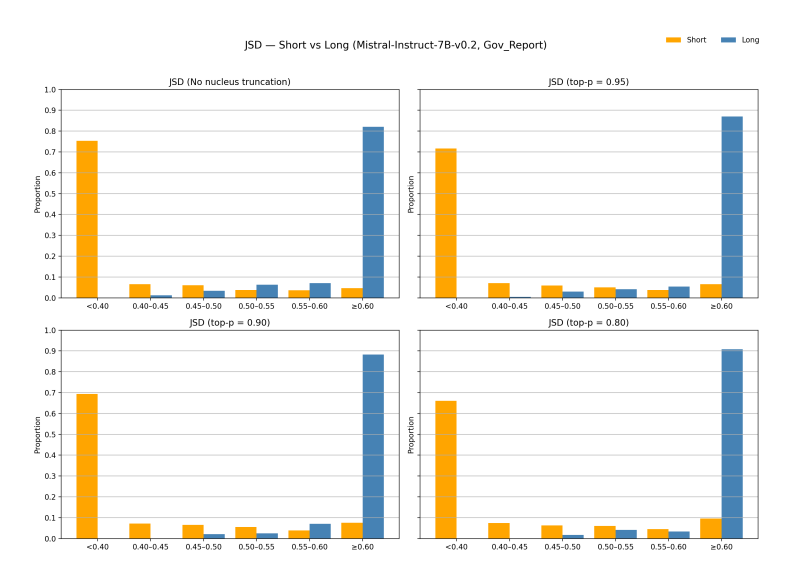


Figure 23: LSDS distribution with Mistral-7B-Instruct-v0.2 on GovReport(5000 samples) with no nucleus sampling, p = 0.95, p = 0.90, and p = 0.80.

long- versus short-context tokens requires balancing correct identification of long-context samples with avoidance of false detections. Thus Youden's J provides an appropriate criterion for threshold selection. Table 5 summarizes the best thresholds and corresponding performance metrics.

Table 5: Ablation study on different nucleus sampling parameters (p). Reported are the optimal threshold, maximized Youden's J, true positive rate (TPR), false positive rate (FPR), precision, recall, and accuracy.

Case	Threshold	J	TPR	FPR	Precision	Recall	Accuracy
No nucleus	0.49	0.834	0.967	0.133	0.268	0.967	87.2%
top-p=0.95	0.53	0.831	0.950	0.119	0.286	0.950	88.4%
top-p=0.90	0.55	0.840	0.954	0.114	0.296	0.954	88.9%
top-p=0.80	0.62	0.816	0.895	0.079	0.361	0.895	91.9%

The setting p=0.90 achieves the highest Youden's J (0.840), indicating the most balanced trade-off between sensitivity (TPR) and specificity (1 – FPR). While p=0.80 achieves the highest accuracy (91.9%), its J value is lower, reflecting weaker overall discriminative balance. Therefore, we adopt p=0.90 as our standard nucleus sampling configuration in the main experiments. This choice is consistent with prior work recommending p in the 0.9–0.95 range for stable yet diverse generation quality (Holtzman et al., 2020).

E.3 ABLATION ON SHORT-CONTEXT LENGTH

We investigate the effect of varying the short-context prefix length ℓ on LSDS and JSD threshold. Experiments are run with Mistral-7B-Instruct-v0.2 on Government Report, using 5000 randomly selected samples, with full context length ranging from 100–1000 tokens. The ground truth oracle we use here is *Prior Work Oracle* as introduced in Sec. 5, and the short prefix length in Equation 2 is adjusted accordingly when computing LSD.

Different fixed short-prefix length. Figure 24 shows results for $\ell=8,16,32,64$. We observe that the overall distributional separation between short and long contexts is preserved across all choices. However, very small short-context prefixes (e.g., $\ell=8$) produce more imbalanced distributions: nearly 20% of short-context tokens fall above the detection threshold. This indicates that while separation is robust, extremely small short prefixes may introduce higher false-positive rates. In

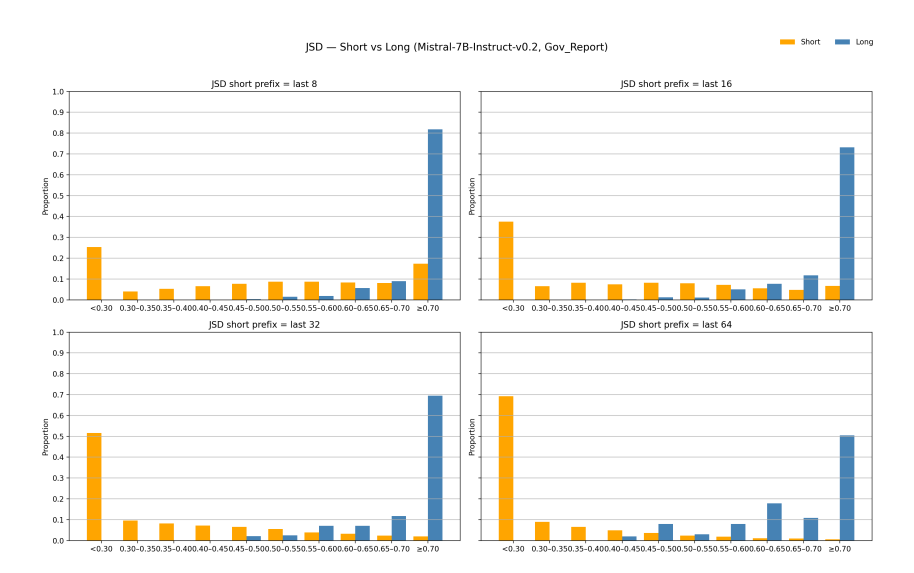


Figure 24: LSDS distribution with Mistral-7B-Instruct-v0.2 on GovReport(5000 samples) with short prefix length $\ell=8,16,32,64$.

contrast, $\ell=32,64$ yield clearer separation, with false negative rates less than 5%, suggesting they are preferable for stable detection. Although using longer prefixes incurs slightly higher computational cost, the improved robustness makes the tradeoff worthwhile—especially in applications where false positives are costly.

Adaptive Short-Context Length. We also evaluate an adaptive strategy where the short-context length is chosen as a proportion of the full sequence length, $\ell=0.1|s|$. Figure 25 demonstrates consistent separation trends under this setup, while adapting naturally to dataset-specific context lengths. Such adaptive schemes may provide better cross-dataset generalization, although their computational implications require further study. We leave exploration of such direction for future work.

Figure 25: LSDS distribution with Mistral-7B-Instruct-v0.2 on GovReport(5000 samples) with short prefix length $\ell=0.1|s|$, consistent separation of the distributions is preserved.

E.4 COMPUTATIONAL OVERHEAD OF LSDS DETECTION AND TABOO

In this section, we quantify the computational cost introduced by LSDS. Recall that LSDS requires evaluating token distributions under both the full co

evaluating token distributions under both the full context and a short suffix (e.g., 32 tokens). For a generation task, the full forward is already computed, so the incremental cost reduces to a single short forward (32 tokens) plus lightweight top-p filtering and JSD computation.

We benchmark this overhead on Qwen2.5 models of different scales (1.5B, 7B, 14B) using contexts $|\mathbf{s}|=100,250,500,1000,2000,4000,6000$. The absolute overhead remained nearly constant: about 35–40 ms for 1.5B, 37–41 ms for 7B, and 58–67 ms for 14B. Relative cost is high at short contexts (> 90% at $|\mathbf{s}|=100$) but drops to $\approx 6-8\%$ at $|\mathbf{s}|=6000$). These results confirm that LSDS adds only minor and predictable overhead with cache reuse.

For other purposes or as a conservative upper bound, one can rerun the full forward pass, which would roughly double the cost. In addition, using adaptive short-prefix length as described above introduces overhead that scales linearly with context length.

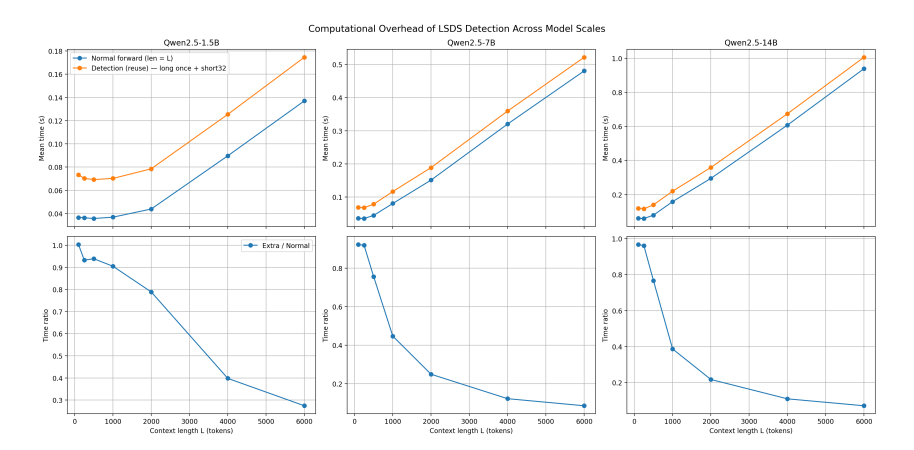


Figure 26: Computational overhead of LSDS detection across Qwen2.5 models (1.5B, 7B, 14B). Top row: mean forward time for normal inference versus detection with reuse (long context + 32-token suffix). Bottom row: relative overhead, measured as the ratio of additional cost to normal forward time. The added cost is nearly constant, demonstrating that LSDS overhead is limited, predictable, and diminishes in importance as sequence length grows.

Figure 26 illustrates the relative computational cost of a full forward pass compared with the extra short-context forward required for detection across all three models.

Regarding the calculations for selecting target tokens, the token selection takes on average less than $\leq 1\%$ of the computation time in comparison to the forward pass, thus we consider it as negligible.

F LONG-CONTEXT TOKEN DETECTION AND BOOSTING

F.1 PROBABILITY SHIFT AS SELECTION METRIC

For our selection of long context relevant tokens, we decide to to use the change in the probability values as our determining metric. While we decide on using the probability difference LSPS $(t|\mathbf{s}) = \mathbf{p}_{p=0.9}(\mathbf{s}_c)(t) - \mathbf{p}_{p=0.9}(\mathbf{s}_{[-32:c]})(t)$ as the determining factor, alternative choice could be the use of probability ratios rather than the difference. In other words we can define **Long-Short Probability Ratio**:

$$\mathsf{LSPR}\left(t|\mathbf{s}\right) = \log(\frac{\mathbf{p}_{p=0.9}(\mathbf{s}_c)(t)}{\mathbf{p}_{p=0.9}(\mathbf{s}_{[-32:c]})(t)})$$

A comparison between this form of metric and our probability difference **LSPS** becomes important when you consider works such as Fang et al. (2025) use the log probability ratio to detect long-short context/next-tokens. Additionally, in Malkin et al. (2022) and Duh et al. (2024) the authors use the log ratio for probability and logits with in the form of $\mathcal{P}_{\mathbf{s}_c}^{1.5}\mathcal{P}_{\mathbf{s}_{[-32:c]}}^{0.5}(t)$ to improve the final probability of long-context tokens. Implicitly, such methods select and increase the probability of tokens who's probability ratio increases rather than the difference itself.

In order to compare the choice of metric, we compare the use of **LSPS** and **LSPR** when boosting the final word/token of on the validation set of LAMBADA (Paperno et al., 2016) dataset. For each context, we have a ground truth next token, which we call the target token \hat{t} . All other tokens we call incorrect tokens. We analyze the choice of which token's are selected for probability increase rather than the improvement itself, therefore we don't include multiplicative factors like λ . For each case of boosting, we consider the following scenarios:

- Scenario 1 (Best): $\hat{t} \in \mathcal{B}$ and $\mathbf{p}_{p=0.9}(\mathbf{s})(\hat{t}) \geq \mathbf{p}_{p=0.9}(\mathbf{s})(t)$ for any other $t \in \mathcal{B}$. Under such a scenario, even if some non answer tokens are selected for probability increase, if we grow λ eventually greedy sampling would select select the answer token.
- Scenario 2 (Bad): $\hat{t} \in \mathcal{B}$ however, there exists at least one token $t \in \mathcal{B}$ with a higher probability than the answer token $\mathbf{p}_{p=0.9}(\mathbf{s})(t) > \mathbf{p}_{p=0.9}(\mathbf{s})(\hat{t}) \ \forall \ t \in \mathcal{B}$. Under such a scenario, while a

higher λ value increases the probability of \hat{t} and thus improving perplexity, but there there isn't a possibility of the ground token to be selected by a greedy sampler.

- Scenario 3 (Worst): $\hat{t} \notin \mathcal{B} \neq \emptyset$. In this case we didn't detect the ground truth token but rather chose a set of incorrect tokens. Under such circumstances, the model next token perplexity would suffer.
- Scenario 4 (Neutral): $\mathcal{B} = \emptyset$ and so no change is made to the probability distribution.

We use nucleus sampling with p=0.9 and set a minimum probability of 10^{-6} as the minimum, in order to prevent numerical instability for the log probability calculations. We will select a range of ϵ values as the selection threshold with respect to the metrics themselves. We report the ratio of each of above's scenarios from the 5153 examples in the LAMBADA validation dataset.

Table 6: Analysis of ground truth \hat{t} token being selected for probability improvement. A comparisong between LSPD (diff) and LSPR (log ratio).

(a) LSPD (diff case)

(b) LSPR (log ratio case)

	. ,	`	,			. ,	` ` ` `		
ϵ	Best	Bad	Worst	Neutral	ϵ	Best	Bad	Worst	Neutral
0.04	66.8%	10.0%	14.2%	9.1%	0.5	60.3%	10.7%	20.2%	8.8%
0.06	65.5%	7.8%	12.8%	13.9%	1.0	57.7%	7.2%	22.1%	13.0%
0.08	64.3%	6.4%	11.1%	18.2%	1.5	56.2%	5.2%	23.1%	15.4%
0.10	62.9%	5.4%	9.5%	22.1%	2.0	54.8%	4.3%	23.9%	17.0%
0.12	61.4%	4.4%	8.6%	25.7%	2.5	53.2%	3.7%	24.8%	18.3%
0.14	59.8%	3.6%	7.7%	28.9%	3.0	51.7%	3.1%	25.8%	19.5%
0.16	58.1%	3.0%	6.8%	32.1%	3.5	49.7%	2.6%	27.5%	20.3%
0.18	56.5%	2.4%	6.1%	35.0%	4.0	46.8%	2.0%	29.4%	21.8%
0.20	55.0%	2.0%	5.6%	37.5%	4.5	43.2%	1.6%	31.5%	23.7%
0.22	53.3%	1.5%	5.1%	40.1%	5.0	38.5%	1.4%	34.2%	26.0%

We observe that using log probability ratio is more likely to lead to a wrong token selection for the boosted set without including the target token \hat{t} . This case is particularly dangerous as it negatively impacts a metric such as perplexity. Additionally, results suggest that the selection performance highly sensitive to the choice of ϵ .

From our analysis such observations can be explained by the sensitivity of log ratio. Particularly for tokens with near zero probability, small perturbation when moving from short to long context probability can be registered under large change in probability ratio changes. Consider using \log_{10} for this explanation only (experiments are done with natural log). If a token's probability goes from $\mathbf{p}_{p=0.9}(\mathbf{s}_{[-32:c]})(t) =$ $10^{-6} \rightarrow \mathbf{p}_{n=0.9}(\mathbf{s})(t) = 10^{-2}$, the log probability ratio is set to 4. Similarly if the token's probability goes from $10^{-3} \rightarrow 10$ we have a similar probability ratio change. However, for the first scenario the full context token probability is near zero, while for the second case the token has a 10% probability. If we go with a the log ratio, both these tokens are treated equally.

On the other hand, for the probability difference case, we have implicitly set a min-

Table 7: XSum summarization results (Average over all generations; Best-per-example in parentheses). Bold = best Average, Underline = best Best-per-example. Regarding the low performance of CAD, we employ the same methods we did for the QA and with a $\alpha=0.5$ hyperparameter selection similar to their setup. Interestingly our average Vanilla Score is similar to theirs. Nevertheless this table is provided to show that our TaBoo method successfully removes certain short context bias in the context of summarization, not to compare our methods directly with CAD.

Model	Method	F1	BLEU	ROUGE-L
LLaMA-2-7B	Vanilla	18.1 (28.6)	2.3 (5.2)	17.4 (27.3)
	CAD	10.4 (16.4)	1.0 (1.6)	10.0 (15.5)
	TaBoo	21.0 (<u>31.5</u>)	3.0 (<u>6.9</u>)	19.9 (<u>30.0</u>)
LLaMA-3-8B	Vanilla	18.4 (29.6)	2.4 (5.9)	17.8 (28.7)
	CAD	12.0 (18.6)	1.1 (2.0)	11.5 (17.5)
	TaBoo	20.7 (<u>31.8</u>)	3.0 (<u>6.9</u>)	19.7 (<u>30.5</u>)
Mistral-8B	Vanilla	18.9 (26.5)	2.4 (4.5)	17.9 (25.1)
	CAD	9.4 (12.8)	0.8 (1.1)	9.2 (12.3)
	TaBoo	21.3 (<u>28.0</u>)	3.1 (<u>5.5</u>)	20.4 (<u>26.7</u>)
Qwen2-7B	Vanilla	20.8 (28.3)	2.7 (5.0)	19.5 (26.7)
	CAD	12.0 (17.3)	1.1 (1.7)	11.5 (16.2)
	TaBoo	21.1 (27.9)	2.7 (4.8)	19.9 (26.2)
Mistral-Inst-8B	Vanilla	24.4 (33.5)	3.9 (8.0)	22.4 (31.4)
	CAD	12.2 (18.4)	1.2 (2.1)	11.3 (17.0)
	TaBoo	25.2 (33.1)	4.4 (7.9)	23.3 (31.0)

imal lower bound on the $\mathbf{p}_{p=0.9}(\mathbf{s})(t) \geq \epsilon$ by only selecting tokens where $|\mathbf{p}_{p=0.9}(\mathbf{s})(t)| - \mathbf{p}_{p=0.9}(\mathbf{s}_{[-32:c]})(t)| \geq \epsilon$. This allows us to circumvent tokens who have very low probability where the log ratio behavior could be noisy and misleading. We believe this is a potential reason for why the long context token selection algorithm in Fang et al. (2025) uses $\log(\mathcal{P}_{\mathbf{s}})(t) \geq 10^{-2}$ (Long-Context Likelihood (LCL)) in addition to their log probability ratio to classify tokens.

While we find probability difference to be a safer and more effective option for our studies, further analysis could help discover new methods for ad-hoc detection of long-context relevant token by comparing short-long context distributions. We believe this can serve a direction for future research.

F.2 TABOO ALGORITHM

 Algorithm 9 presents our TaBoo method.

Algorithm 1: Long Context Token Boosting with JSD and Nucleus Constraint

```
Input: Short- and full-context distributions \mathbf{p}_{\phi}(\mathbf{s}_{[-32:]}), \mathbf{p}_{\phi}(\mathbf{s}); thresholds \epsilon, \gamma; boost factor \lambda; decoding \phi: nucleus sampling with parameter p; support set \mathcal{V}^{\text{nuc}} of \mathbf{p}_{\phi}(\mathbf{s})

Output: TaBoo distribution \widetilde{\mathbf{p}}_{\phi}(\mathbf{s})

Initialize (to the raw probability distribution): \widetilde{\mathbf{p}}(\mathbf{s}) \leftarrow \mathbf{p}_{\phi}(\mathbf{s});

Step 1: Identify whether sequece is long-context:

if LSDS (\mathbf{s}) \leq \gamma then

\mathbf{return} \ \mathbf{p}_{\phi}(\mathbf{s}); // Return unmodified nucleus distribution

Step 2: Identify set of long-context-relevant tokens: \mathcal{B} \leftarrow \{t \in \mathcal{V}^{\text{nuc}} \mid \text{LSPS}(t|\mathbf{s}) > \epsilon\};

Step 3: Targeted Boosting: foreach token t \in \mathcal{B} do

\mathbf{r}_{\phi}(\mathbf{s}) \mid_{t} \leftarrow \lambda \cdot [\mathbf{p}_{\phi}(\mathbf{s})]_{t};

Re-normalize and apply nucleus decoding: \widetilde{\mathbf{p}}(\mathbf{s}) \stackrel{\text{nuc}}{\leftarrow} \widetilde{\mathbf{p}}(\mathbf{s}) / \text{sum}(\widetilde{\mathbf{p}}(\mathbf{s})) for all t \in \mathcal{V};

return \widetilde{\mathbf{p}}(\mathbf{s})
```

F.3 IMPACT OF DECODING

Another question we ask is the impact of using decoding methods when implementing the token selection during Taboo. In order to test this our, we provide a similar table to Tab . 6 but this time without any nucleus sampling and using the raw probability distributions.

Results are provided in Tab . 8. Comparing LSPS we don't observe a major change, one case being better than the other depending on the value of ϵ . For LSPR on the other hand, we can see that not doing any nucleus sampling leads to much more **Worst** case scenarios where we don't boost the answer token but rather a irrelevant one. This observation both points towards the robustness of LSPS w.r.t the next token probability distribution (with or without decoding). Additionally it points our the potential problem with using the log ratio of probabilities.

Table 8: Similar setup to Tab. 6 but this time without any nucleus sampling.

(a) LSPD (diff case)					(b) LSPR (log ratio case)					
ϵ	Best	Bad	Worst	Neutral	 ϵ	Best	Bad	Worst	Neutral	
0.04	66.7%	9.3%	13.8%	9.1%	0.5	60.6%	11.2%	28.1%	0.1%	
0.06	65.4%	7.4%	12.0%	15.2%	1.0	58.5%	7.5%	34.6%	0.3%	
0.08	63.9%	5.9%	10.2%	20.0%	1.5	57.0%	5.4%	38.0%	0.4%	
0.10	62.0%	4.9%	8.7%	24.0%	2.0	55.6%	4.3%	40.4%	0.5%	
0.12	60.3%	3.9%	7.7%	28.1%	2.5	54.0%	3.6%	42.7%	0.6%	
0.14	58.6%	3.2%	6.6%	31.7%	3.0	52.4%	3.0%	45.0%	0.7%	
0.16	56.9%	2.6%	5.9%	34.7%	3.5	50.3%	2.4%	47.9%	0.7%	
0.18	55.2%	2.1%	5.2%	37.6%	4.0	47.3%	1.7%	51.6%	0.8%	
0.20	53.6%	1.6%	4.8%	40.9%	4.5	43.8%	1.3%	56.4%	0.9%	
0.22	51.9%	1.2%	4.3%	42.6%	 5.0	39.0%	1.0%	61.7%	0.9%	

F.4 ILLUSTRATIVE EXAMPLE OF LONG-CONTEXT TOKEN BOOSTING ON NARRATIVEQA

Figure 27 shows some examples from the NARRATIVEQA dataset to illustrate how our boosting method (Taboo) operates.

The boosted output generated by Taboo matches the ground truth, with tokens highlighted by context origin: orange tokens correspond to short-context (names from the question), while blue tokens correspond to long-context (the reasoning required from the story). The figure also shows which tokens were boosted, showing that the algorithm consistently promotes the correct words needed to form the right answer. This example illustrates how Taboo leverages long-context signals to reinforce accurate completions.

F.5 AVERAGE PERFORMANCE WITH STANDARD ERRORS

We report the Average scores for F1, BLEU, and ROUGE-L across all generations; values in parentheses are the corresponding standard errors (SE). These SEs capture variability across evaluation examples on the same split. Results for LLaMA-2-7B on MultifieldQA-en are omitted due to the 4096-token context limit.

Table 9: F1, BLEU, and ROUGE-L (Average; standard error in parentheses). Bold = best Average within each dataset block.

Model	Method	NarrativeQA				HotpotQA			MultifieldQA-en		
		Fl(†)	BLEU(↑)	ROUGE-L(↑)	Fl(↑)	BLEU(↑)	ROUGE-L(↑)	F1(↑)	BLEU(↑)	ROUGE-L(↑)	
LLaMA-2-7B	Vanilla	16.1 (±0.29)	2.9 (±0.09)	22.4 (±0.36)	25.2 (±0.48)	7.7 (±0.21)	32.5 (±0.53)	NA	NA	NA	
	CAD	22.5 (±0.40)	4.3 (±0.12)	30.7 (±0.48)	28.3 (±0.53)	8.5 (±0.24)	34.3 (±0.56)	NA	NA	NA	
	TaBoo	24.1 (±0.41)	4.9 (±0.14)	31.7 (±0.47)	32.8 (±0.58)	10.3 (±0.27)	39.6 (±0.61)	NA	NA	NA	
LLaMA-3-8B	Vanilla	24.0 (±0.37)	4.9 (±0.13)	32.7 (±0.46)	29.2 (±0.49)	9.0 (±0.23)	41.6 (±0.58)	9.9 (±1.62)	7.7(±1.17)	24.0 (±1.73)	
	CAD	35.4 (±0.52)	7.3 (±0.18)	49.4 (±0.62)	27.7 (±0.53)	8.5 (±0.23)	46.9 (±0.68)	18.8 (±1.72)	6.4 (±1.03)	26.2 (±2.02)	
	TaBoo	32.0 (±0.47)	7.2 (±0.18)	42.3 (±0.53)	33.1 (±0.55)	10.6 (±0.26)	48.1 (±0.64)	21.9 (±1.74)	9.1 (±1.29)	28.2 (±1.87)	
Mistral-7B-v0.1	Vanilla	25.7 (±0.41)	5.1 (±0.13)	33.7 (±0.48)	33.0 (±0.54)	10.1 (±0.24)	43.1 (±0.59)	20.6 (±1.54)	6.9 (±1.07)	26.0 (±1.72)	
	CAD	34.3 (±0.55)	7.1 (±0.17)	43.1 (±0.57)	35.9 (±0.62)	11.0 (±0.28)	41.6 (±0.63)	18.8 (±1.44)	5.9 (±0.99)	24.9 (±1.65)	
	TaBoo	35.3 (±0.52)	7.7 (±0.15)	44.4 (±0.46)	37.1 (±0.61)	11.7 (±0.29)	46.3 (±0.64)	23.0 (±1.65)	8.6 (±1.27)	29.5 (±1.83)	
Qwen2-7B	Vanilla	33.6 (±0.49)	8.1 (±0.19)	42.4 (±0.53)	59.4 (±0.64)	20.1 (±0.36)	62.9 (±0.63)	31.1 (±1.86)	15.1 (±1.63)	41.3 (±2.01)	
	CAD	36.6 (±0.58)	8.8 (±0.22)	45.3 (±0.60)	59.3 (±0.68)	20.5 (±0.39)	62.2 (±0.67)	30.6 (±1.80)	14.0 (±1.49)	40.0 (±2.10)	
	TaBoo	38.5 (±0.56)	9.7 (±0.15)	48.2 (±0.64)	63.2 (±0.67)	21.7 (±0.39)	66.6 (±0.65)	32.3 (±1.85)	15.3 (±1.64)	42.3 (±2.07)	

1669

```
1621
1622
1623
1624
                             With supplies of petroleum nearly exhausted in the near future...Wez manages to board the truck and attack Max, but a head-on collision
1625
                                                                 ez and Humungus. Max loses control of the tanker and it rolls off the road. As the injured Max carries the
                             Feral Kid from the wrecked tanker, he sees not petrol, but sand, leaking from the tank. The truck and its trailer are thus exposed as a
1626
                             decoy, allowing the other settlers to escape with the precious fuel in oil drums inside their vehicles. With Pappagallo dead, the Gyro
1627
                             Captain succeeds him as their chief and leads the settlers to the coast, where they establish the "Great Northern Tribe". Max remains
                             alone in the desert, once again becoming a drifter. Years later, the Feral Kid, now the Northern Tribe's new leader (voice by Harold
1628
                             Baigent), reminisces about the legend of the mythical "Road Warrior" (Max) who now exists only in distant memory.
1629
1630
                             Question:
1631
                             What ends up killing wez and humungus?
1632
                             Ground Truth Answer:
1633
                             Wez and Humungus die in a head on collison with Humungus's car
1634
1635
                             Taboo Result:
                             a head-on collision with Humungus's car kills both Wez and Humungus
1636
1637
                                            boost tokens = ['a', 'A'],
                              'head' :
                                           boost tokens = ['head'],
1638
                                            boost tokens = ['-on'],
                              'collision'
                                           boost tokens = ['collision'],
                              'with'
                                           boost tokens = ['with'],
                                           boost tokens = ['hum', 'Hum']
boost tokens = ["'s", '' s']
1640
                                           boost tokens = ['car'],
boost tokens = ['.', '', 'kills', '<|endoftext|>']
1641
                              'kills' :
1642
                                           boost tokens = ['both'],
                                           boost tokens = ['with'].
1643
                                           boost tokens = ['.', '<| endoftext|>']
1644
1645
1646
                             Samantha Caine (Geena Davis) is a schoolteacher in the small town of Honesdale, Pennsylvania, with her boyfriend Hal (Tom Amandes)
1647
                             and her daughter Caitlin (Yvonne Zima). Eight years earlier, she was found washed ashore on a New Jersey beach, pregnant with Caitlin
1648
                             and totally amnesiac. Having never remembered her real name or any part of her life from before that day, "Samantha" has hired a
                            number of private investigators to try to discover her past, the latest being Mitch Henessey (Samuel L. Jackson) ... In the epilogue, Charly has returned to her assumed identity of Samantha Caine, moving with Caitlin and Hal to a remote farmhouse with a bunch of goats, and
1649
1650
                             declines an offer from the president to rejoin the CIA. For his part, Mitch enjoys the publicity attracted by his role in the crisis, and is last
                             seen being interviewed by Larry King on television, where they discuss Perkins, who was indicted for treason.
1651
1652
1653
                             Question:
                             Where was samantha washed ashore eight years earlier?
1655
                             Ground Truth Answer:
                             New Jersey
1656
1657
                             Taboo Result:
1658
                             "Samantha" was found washed ashore on a New Jersey beach, eight years earlier.
1659
                                           boost tokens = ['The', 'Sam'],
1660
                              'Sam':
                                           boost tokens = ['Sam'],
                                            boost tokens = ['Ca', '"'].
1661
                              'was'
                                           boost tokens = ['(', 'was']
                                            boost tokens = ['was', 'found', 'hes'],
                               'found'
1662
                              'was'
                                           boost tokens = ['was'],
                                           boost tokens = ['on'],
1663
                                            boost tokens = ['a'].
                                           boost tokens = ['New'],
1664
                              'New '
                              'Jersey
                                            boost tokens = ['Jersey'],
1665
                                           boost tokens = ['.', ','],
                              'eight' :
                                           boost tokens = ['pre', 'near'],
1666
                              'earlier':
                                           boost tokens = ['prior']
1667
1668
```

Figure 27: Example from NarrativeQA with Taboo. Orange tokens are short-context (names from the question), blue tokens are long-context (story-based reasoning). Boosted tokens align with the correct answer, showing that Taboo consistently promotes the right completions.